U.S. Department
of Transportation
National Highway
Traffic Safety
Administration

www.nhtsa.gov

DOT HS 811 995 May 2014

Development of NHTSA's Side Impact Test Procedure for Child Restraint Systems Using a Deceleration Sled

Final Report
Part 2

DISCLAIMER

Suggested APA Format Citation:

Brelin-Fornari, J., & Janca, S. (2014, May). *Development of NHTSA's side impact test procedure for child restraint systems using a deceleration sled: final report, part 2* (Report No. DOT HS 811 995). Washington, DC: National Highway Traffic Safety Administration.

1. Report No.	2. Government Accession No.	3. Recipient's Catalog No.
DOT HS 811 995		

4. Title and Subtitle	5. Report Date
Development of NHTSA's Side Impact Test Procedure for Child Restraint Systems Using a Deceleration Sled: Final Report, Part 2	May 2014
	6. Performing Organization Code Kettering University Crash Safety Center
7. Author(s) Janet Brelin-Fornari, Ph.D., PE, Director Sheryl Janca, Project Engineer	8. Performing Organization Report No. DOT SIDE_019-DOT_SID_ 038
9. Performing Organization Name and Address Kettering University Crash Safety Center 1700 W. University Ave. Flint, MI 48504	10. Work Unit No. (TRAIS) 11. Contract or Grant No. DTNH22-11-C-00204
12. Sponsoring Agency Name and Address National Highway Traffic Safety Administration 1200 New Jersey Avenue SE. Washington, DC 20590	13. Type of Report and Period Covered Research and Development August 2012 – August 2013 14. Sponsoring Agency Code

15. Supplementary Notes

16. Abstract

This report presents the results of the continued research and development of child seat side impact tests using the deceleration sled at Kettering University's Crash Safety Center. The objective of this test series was to gain further insight into the sensitivity of the side impact test fixture response. Test variations included speed of impact, weight of the fixture, and impact characteristics. Additionally, 20 child restraint system (CRS) specific tests were conducted using a fixed set of test parameters.

17. Key Word	18. Distribution Statement
Side impact development, child restraint system, deceleration sled	Document is available to the public from the Technical Information Service www.ntis.gov

19. Security Classif. (of this report)	20. Security Classif. (of this page)	21. No. of Pages	22. Price
		62	

Table of Contents

1.0 Technical Plan

Per contract DTNH22-11-C-00204 Modifications III to V, the Kettering University Crash Safety Center (KCS) was tasked to:

1. Modify the side impact test fixture to address the design issues identified during the Phase I tests;
2. Conduct 15 baseline tests to assess the viability of the modifications of the fixture, the pre-impact kinematics of the anthropomorphic test device (ATD) head, and the measurement of the impact speed of the secondary carriage with the door fixture;
3. Conduct deceleration sled tests to assess repeatability;
4. Conduct 8 child restraint system (CRS) specific tests with a secondary carriage weight of 102 kg (225 lb);
5. Conduct 6 baseline tests to assess the secondary carriage acceleration and velocity time history with varying secondary carriage weight, aluminum honeycomb volume, and impact plane alignment;
6. Conduct 12 CRS specific tests with a secondary carriage weight of 116 kg (256 lb); and
7. Analyze, transfer, and report test data.

2.0 Test Fixture Specifications and Modifications

The side impact test fixture was fabricated during Phase I of the contract and based on the fixture housed at the National Highway Traffic Safety Administration Vehicle Research and Test Center (VRTC) in East Liberty, Ohio. The fixture consists of two distinct parts: the primary carriage and the secondary carriage (Figure 1). The primary carriage is fixed to the bedplate of the deceleration sled and consists of the fixture base plate, door fixture (with foams), aluminum honeycomb, and an anti-rebound mechanism. The secondary carriage is free to move on a set of linear bearings affixed to the primary carriage base plate. The secondary carriage consists of the generic vehicle seat (with foam and cover), the CRS being tested, and the test ATD. The side impact fixture is attached to the sled mechanism at a 10 degree angle with respect to the forward motion of the driven sled (Figure 2).

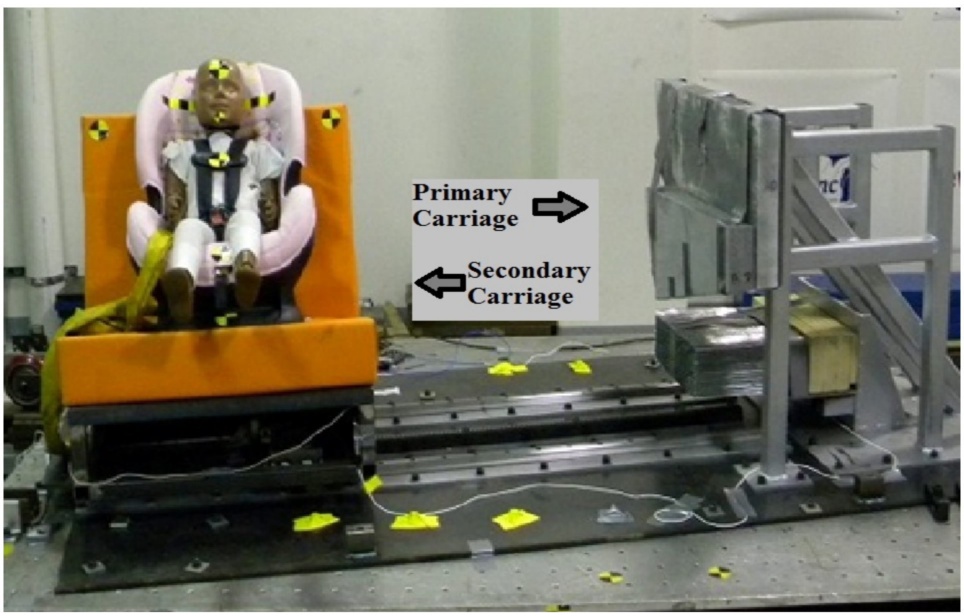

Figure 1: Side view of the side impact fixture attached to the deceleration sled

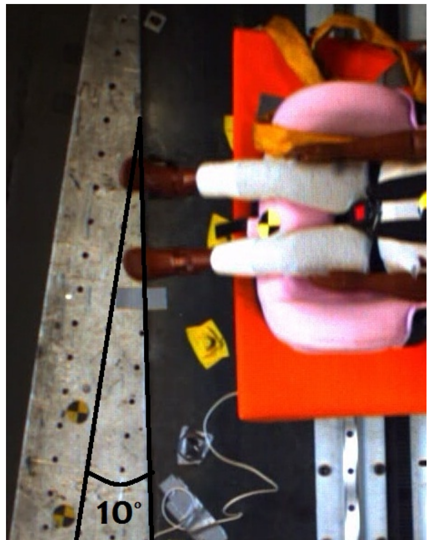

Door Impact End

Figure 2: Depiction of the 10º secondary carriage CCW rotation angle with respect to the longitudinal axis of the primary carriage (not to scale)

Material specifications for the fixture:

- Door foam backing: Ethafoam 220, 51 mm ± 3 mm (2.0 in ± 0.1 in) thickness (Figure 3)
- "Armrest" door foam: Four (4) pound gray foam from United Foam (UF), 64 mm ± 3 mm (2.5 in ± 0.1 in) thickness (Figure 3)
- Foams were attached using 3M two-sided foam mounting tape.
- Aluminum Honeycomb PAMG-XR1 5052 from Plascore: Test size of 305 mm (depth) x 343 mm x 127 mm ± 6 mm (12" x 13.5" x 5" ± 0.2 in)
- ECE R-44 bench foam modified to fit the seat back and bottom of the side impact fixture bench
- ECE R-44 cloth bench foam covering formed to fit the bench foam

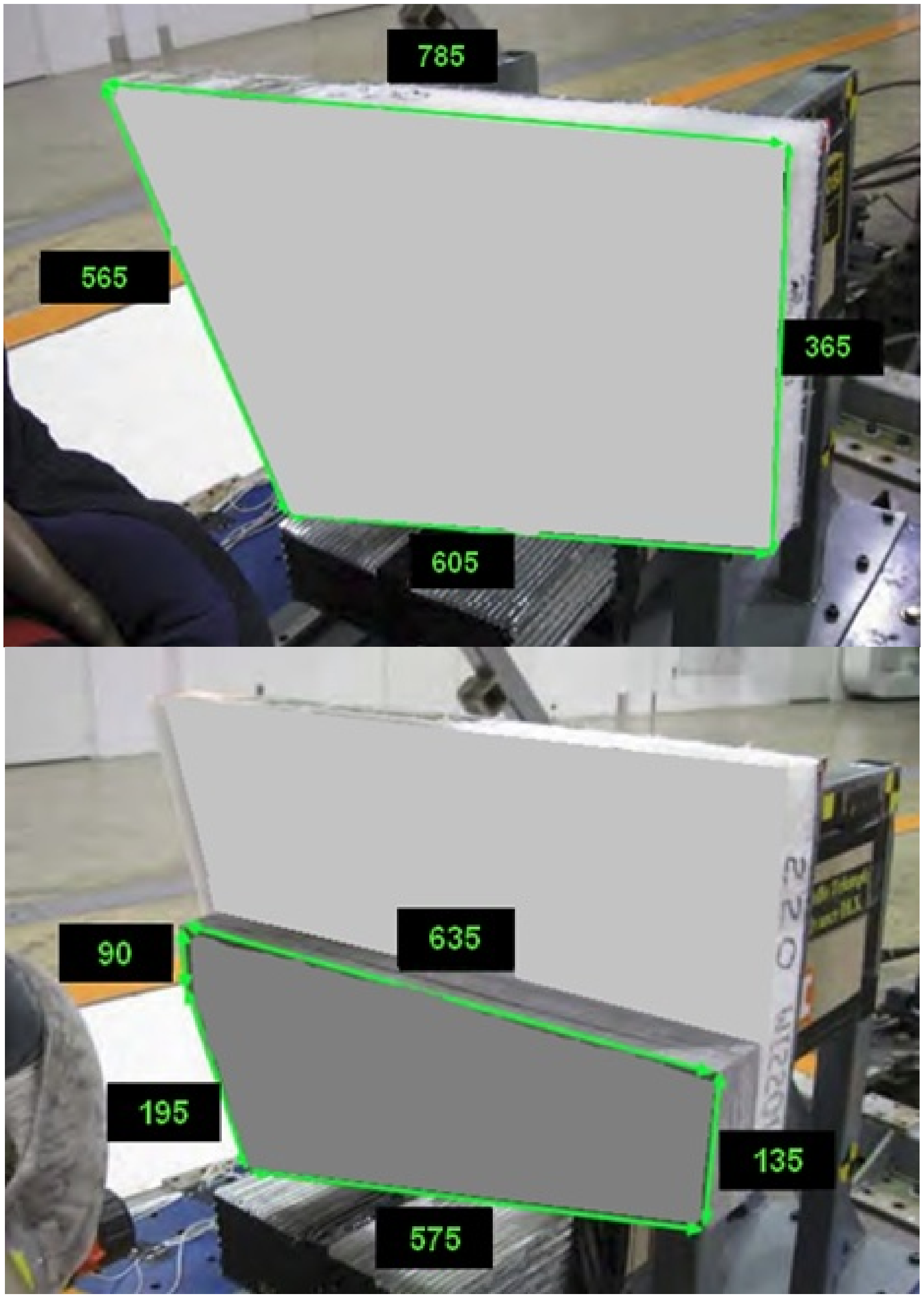

Figure 3: Door foam dimensions (mm) ± 6 mm

The original side impact test fixture was fabricated and tested in Phase I of the contract. Included in the scope of contract Modification III, the fixture was changed to include an alternate anti-rebound mechanism, solid support structure for the aluminum honeycomb, uniform honeycomb impact plate, modified seat back pan, and raised lower anchor attachment points.

In the previous version of the test fixture, a ratchet and pawl system was attached to the secondary carriage to prevent its rebound after impact. The 11.8 kg (26 lb) mechanism was removed and replaced with a pop-up pedal device attached to the primary carriage (Figure 4). The pedal device is staged by depressing the lower mounted springs and sliding the secondary carriage overtop. During the test, the secondary carriage moves 800 mm with respect to the primary carriage, prior to impact with the wall. To reduce friction during this run-up, the top pedal surface slides against a Delrin coating fastened to the underside of the secondary carriage. Once the secondary carriage surpasses the end of the pedal (prior to impact with the wall), the pedal pops-up to stop the secondary carriage from rebounding. To limit the pedal pop-up angle, a strap is affixed to the pivot end of the cantilevered plate.

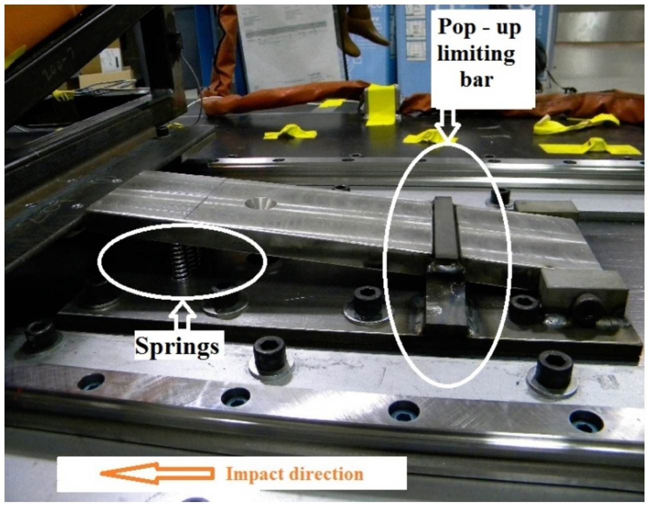

Figure 4: Pop-up pedal device used to prevent post impact rebound (shown post impact)

In the previous version of the test fixture, a wooden support structure was inserted behind the aluminum honeycomb on the primary carriage. For this series, the wooden support structure was removed and replaced with a steel support. Spacing between the door foam face impact plane and the honeycomb support plate was set at 347 mm (Figure 5). This distance includes the prescribed 305 mm depth of an aluminum honeycomb test piece. Therefore, the distance from the door foam face impact plane to the honeycomb face impact plane is 42 mm (347 mm – 305 mm).

Besides the removal of the ratchet and pawl mechanism from the secondary carriage, three other modifications were made to the secondary carriage structure.

- The two larger holes in the original aluminum honeycombing striking plate were reduced to match the size of the other holes in the plate (Figure 6).
- The lower anchors of the Lower Anchors and Tether for Children (LATCH) mechanism were raised from the Phase I location (Figure 6).
- A 12 mm tall notch was made in the seat back pan above the lower anchor bracket (Figure 7).

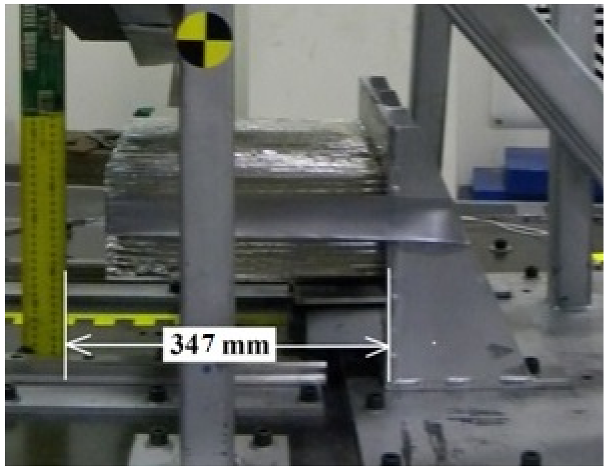

Figure 5: Aluminum honeycomb support structure

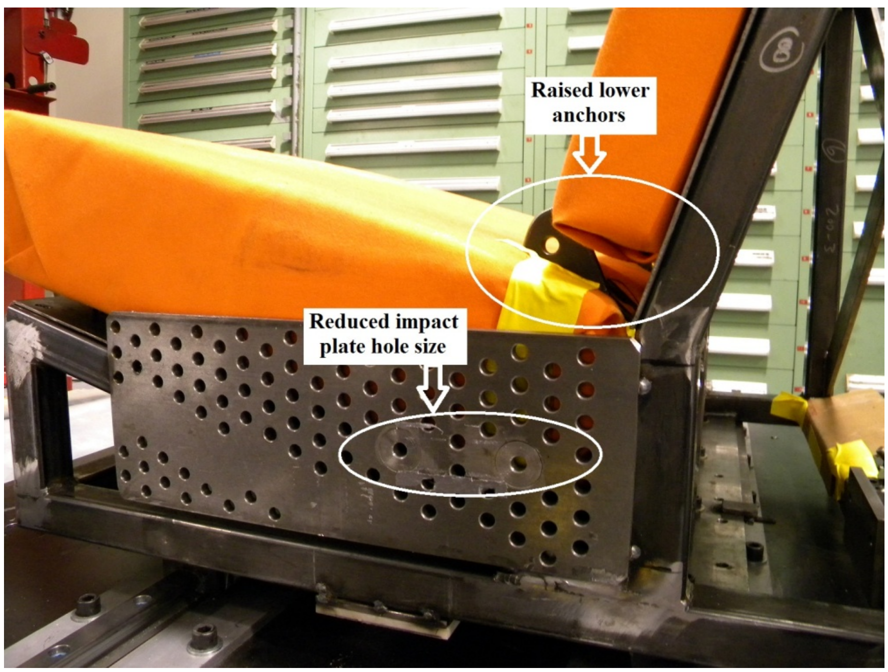

Figure 6: Modifications to the aluminum honeycomb striking plate and the lower anchor attachment brackets

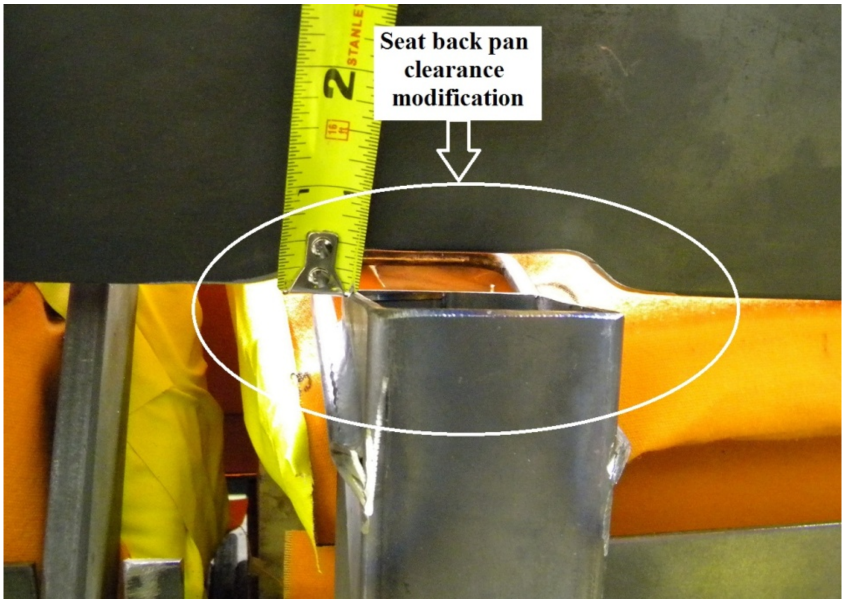

Figure 7: Modification to the seat back pan

This version of the modified test fixture was used for Baseline I and Tests 019 to 026. The weight of the total fixture, primary and secondary carriages, was 631 kg (1391 lb). The secondary carriage alone weighed 104 kg (229 lb). The secondary carriage weighed less than it did during tests 001 to 018 conducted in Phase I of the contract due to the modifications made to the secondary carriage as previously described. After further assessment (Section 6.3), ballast was added to the secondary carriage to increase its weight to 116 kg (256 lb). The 116 kg secondary carriage was used for Tests 027 to 038. (Table 1)

Table 1: Weight of the secondary carriage for the tests in the series

Test Numbers	Secondary Carriage Weight (kg) (lb)
001 - 018	114 (251)
019 - 026	104 (229)
027 - 038	116 (256)

3.0 Overview of Deceleration Sled Test

For all tests, the secondary carriage was staged 800 mm ± 6 mm from the honeycomb face. The centerline of the CRS, whether forward facing or rear facing, was set at 300 mm ± 6 mm from the left side bench edge (Figure 8).

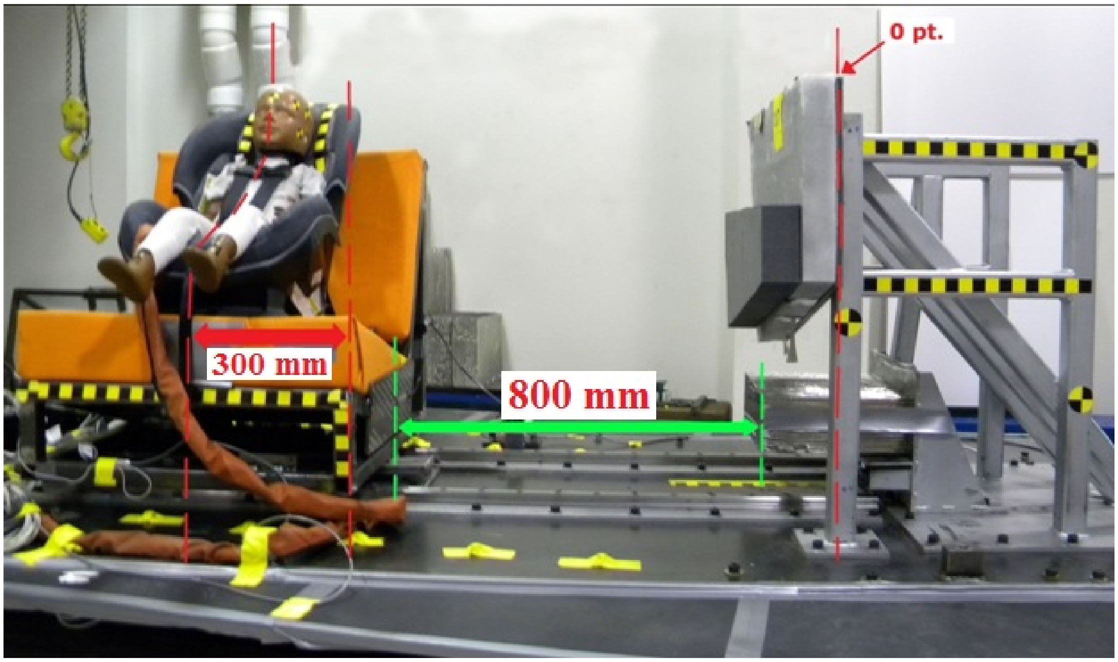

Figure 8: Alignment of the fixture attributes at time zero

In general, when using the fixture on the deceleration sled, both the primary and secondary carriages start from rest. The complete fixture is propelled to the impact end of the sled, attaining a speed of nearly 21 miles per hour. At impact with the decelerator, the primary carriage is brought to rest in 135 milliseconds. During this time, the secondary carriage is free to continue to move on the linear bearings with an initial speed of ~20 mph. Due to friction along the linear rails, the secondary carriage (CRS/vehicle seat) impacts the primary carriage (door/honeycomb) at a reduced speed of ~ 19 mph.

3.1 ATD Installation and ATD Instrumentation

The test series called for a total of 20 tests using two different ATDs: 7 tests with the Child Restraint/Air Bag Interaction 12-month-old (CRABI 12) and 13 tests with the Q3s. The instrumentation for the ATDs is listed in Table 2. The instrumentation for the CRABI 12 was supplied by the KCS and calibrated in accordance with the protocol specified in NHTSA "Laboratory Test Procedure for FMVSS No. 213, Child Restraint Systems" (TP-213-09 June 7, 2006). The instrumentation for the Q3s was supplied by NHTSA VRTC along with the ATD. The CRABI 12 was clothed as specified in TP-213-09. The ATDs were chalk painted on the impact side of the head using contrasting colors to distinguish the front, side, and top of the head. Additionally, copper mesh covered the ATD's head for use with a door contact switch.

Table 2: ATD instrumentation

Instrumentation Channel	**Q3s (number of channels)**	**CRABI 12 (number of channels)**
Head triaxial accelerometer (cg) A_x, A_y, A_z	3	3
Neck upper load cell Forces Fx, Fy, Fz Moment Mx, My, Mz	 3 3	 3 3
Shoulder displacement D_y	1	-
Chest triaxial accelerometer A_x, A_y, A_z	-	3
IR-TRACC displacement D_y	1	-
Spine triaxial accelerometer A_x, A_y, A_z	3	-
Lumbar spine load cell Forces Fx, Fy, Fz Moment Mx, My, Mz	 3 3	 3 3
Pubic force F_y	1	-
Pelvis triaxial accelerometer (cg) A_x, A_y, A_z	3	3
Total	**24**	**21**

3.2 Sled and Buck Instrumentation

The deceleration sled and the test buck had 16 channels of instrumentation (Table 3). Of those channels: 12 were acceleration, 1 was velocity, 1 was force, and 2 were voltage. The accelerometer locations are depicted in Figure 9. A positive contact switch was used between the head of the ATD and the door to determine if contact was made between the two during impact. A wire mesh cover was placed over the ATD head and foil tape (McMaster-Carr p/n 761A62, .005” thick by 6” width) was secured to the surface of the door foam. A positive contact switch was added between the honeycomb striking plate and the aluminum honeycomb block beginning with Test 027. A strobe light switch was in place and visible in all high-speed videos indicating the contact between the honeycomb striking plate and the aluminum honeycomb block.

Table 3: Sled and fixture instrumentation

Position of Measurement	**Type of measurement**	**Number of channels**
(1)* Primary carriage A_x	Linear acceleration	1
(2) Primary carriage A_x, A_y, A_z	Linear acceleration	3
(3) Bench seat back A_x, A_y	Linear acceleration	2
(4) Bench seat base A_x	Linear acceleration	1
Velocity secondary carriage (bench seat) t	time	1
(6) Rigid wall on primary carriage A_x, A_y	Linear acceleration	2
(7) CRS back A_x, A_y, A_z	Linear acceleration	3
Top tether (when applied) F_z	Axial belt force	1
Head contact indication switch V	Voltage	1
Honeycomb contact indication switch** V	Voltage	1
Total instrumentation on sled and fixture		**16**

* Numbers correspond to labels on Figure 9

**The honeycomb contact switch was added for Tests 027 to 038

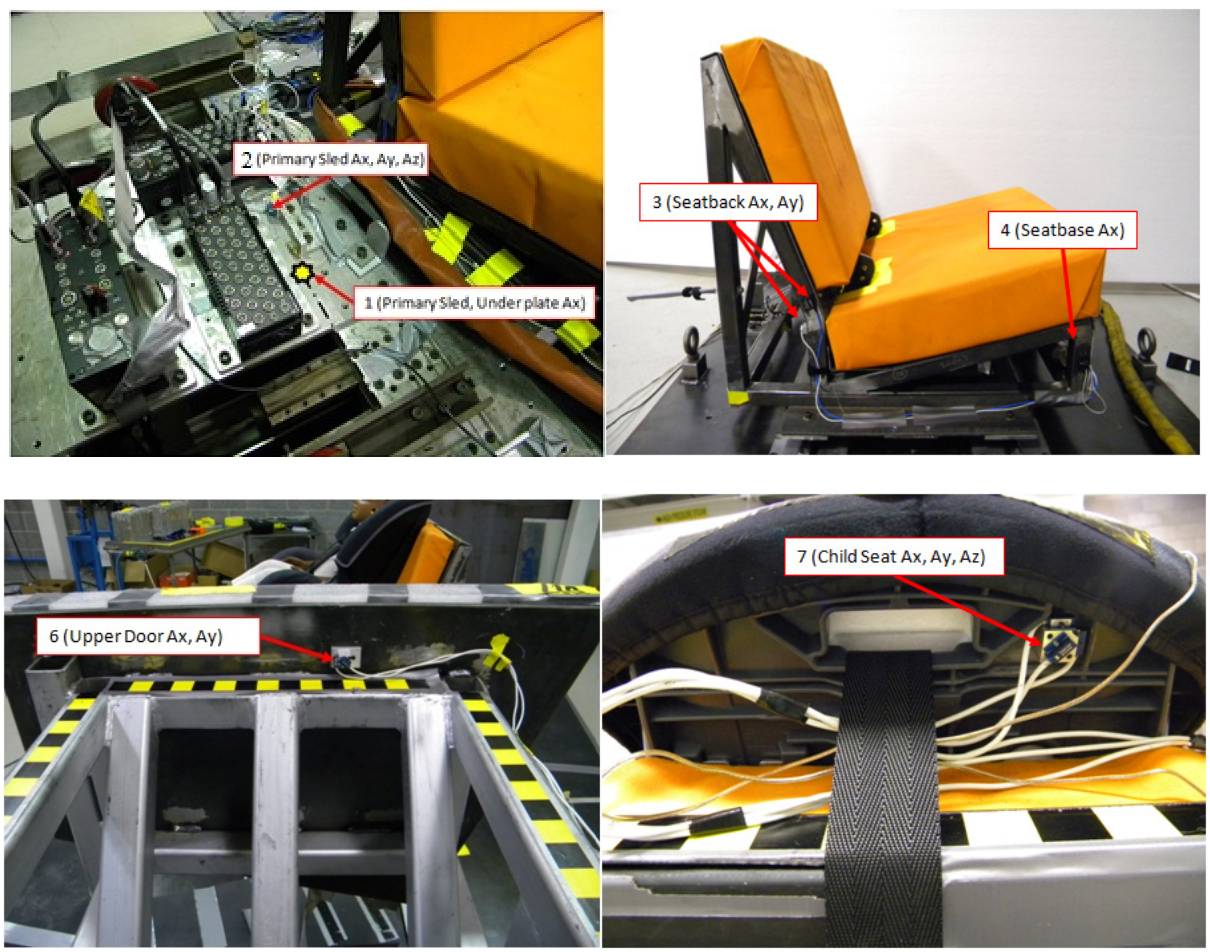

Figure 9: Instrumentation locations

3.3 Still Photos and High-Speed Video Cameras

Five high-speed, color video cameras were used to record the event (Table 4). All the cameras were stationary since the primary carriage is not moving during the impact of the secondary carriage to the door (Figure 10).

Table 4: Camera specifications

Camera	Location	Lens	Type
CAMOH	Overhead 1 (wide view)	20 mm	Photron PCI
CAM1	Overhead 2 (tight view)	6 mm	Photron MH4
CAM2	Front	12 mm	Photron MH4
CAM3	In-Line with Secondary Carriage	3.5 mm	Photron MH4
CAM4	Front Oblique (forward facing)	12 mm	Photron MH4
CAM4	Door surface (rearward facing)	12 mm	Photron MH4

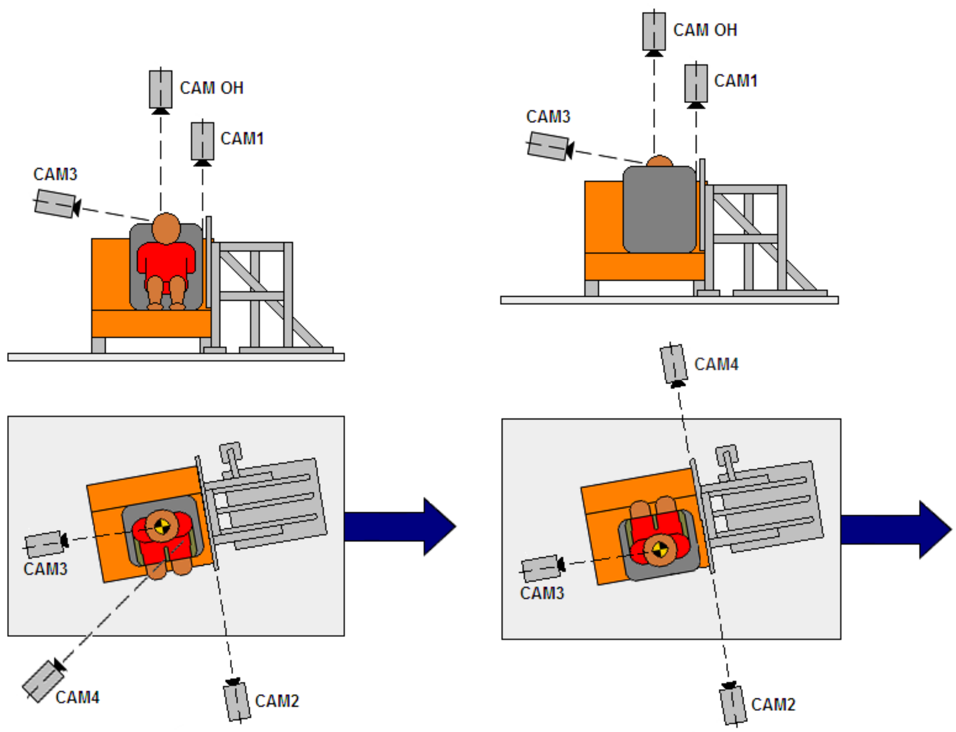

Figure 10: Camera positioning for forward facing CRS and rearward facing CRS tests

Pre- and post-test photos were taken per specifications in TP-213-09 and supplied with the individual test reports.

A strobe light was triggered by the secondary carriage impact into the aluminum honeycomb block and visible in all camera views.

4.0 Baseline Testing: Part I

The objective of the Baseline I Test Series was to determine the viability of the changes made to the test fixture, to assess the kinematics of the ATD head pre-impact, and to evaluate a range of CRS-to-door impact speeds. The goals of the test series were achieved.

4.1 Viability of Fixture Changes

The fixture was modified to include an alternate anti-rebound mechanism, solid support structure for the aluminum honeycomb, uniform honeycomb impact plate, modified seat back pan, and raised lower anchor attachment points.

The modified anti-rebound mechanism performed as designed except for one baseline test. In each test, it can be seen in the high-speed video that the pedal mechanism vibrates on the lower springs after it pops up from the depressed position. In Baseline Test 5, the rebounding secondary carriage moved past the pedal mechanism while it was on a downward motion in the vibration oscillation. The secondary carriage came to rest before impacting the stops at the end of the rails. This event did not alter the impact of the CRS to the door. But, in order to address the issue, longer springs (30 mm to 44 mm) were inserted into the pedal mechanism for all remaining tests.

In Phase I of the testing it was reported that there was test-to-test variation of crush in the aluminum honeycomb including an irregular crush profile across the face of the impacted edge. The new solid support structure for the aluminum honeycomb and the consistent hole-size on the honeycomb impact plate resolved the issue (Figure 11). The struck honeycomb material deformed uniformly (Figure 12) with the crush primarily on the impacted end. Also, the resulting crush was regular for equivalent impact speeds, with 135 mm (5.3 inches) of crush recorded for an impact velocity of 31.3 kph (Baseline Tests 16 and 17).

The modification to the lower anchors of the LATCH mechanism performed as designed. The CRS belt attachments were able to be installed per the manufacturer's requirements and test protocol.

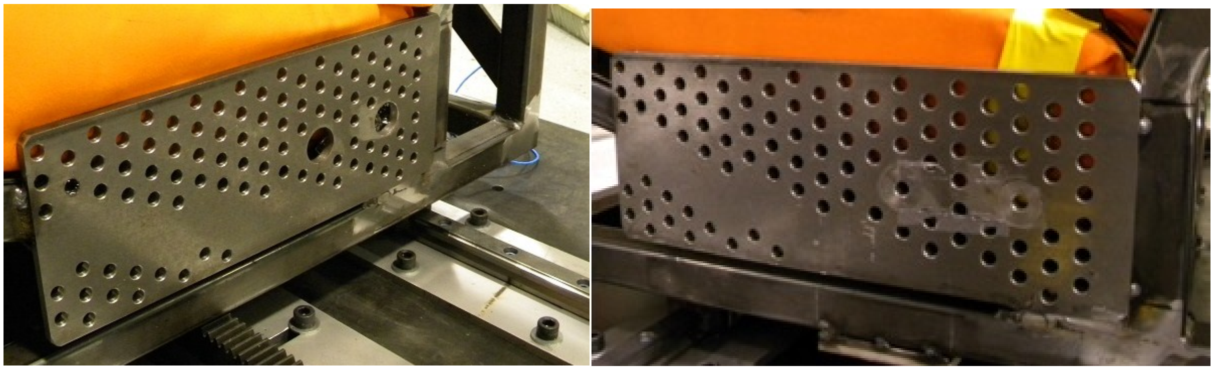

Phase I Test Series Current Test Series

Figure 11: Honeycomb impact plate Phase I of the test series and for Baseline I test series

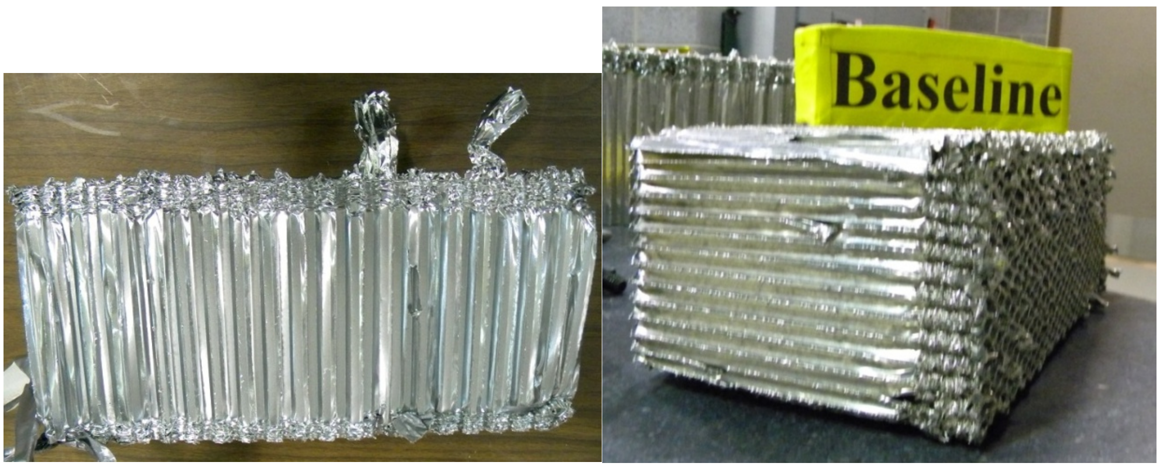

Phase I Test Series Current Test Series

Figure 12: Crushed honeycomb from Phase I of the test series and for Baseline I test series

4.2 Kinematic Analysis of ATD Head

In Phase I of the testing, it was reported that the ATD head flexed forward during the 800 mm run-up of the secondary carriage from the initial staged position to impact with the foam door face (Figure 13). In Baseline I series, the ATD and the CRS were targeted and inch-taped to allow for measurement of the motion. When the head was allowed to move with no restriction during the 800 mm run-up prior to CRS impact, the head had a maximum forward linear displacement of 85 mm (3.3 inches), limited by the ATD neck bumpers. Prior to impact of the CRS with the door, the head moved 10 mm (0.4 inches) rearward from this maximum position.

In seven (7) of the tests, a piece of 1 inch wide, 3M masking tape was secured to the head of the ATD on one end and the back of the CRS on the other. The tape was secured to the head in the neutral position (no forced flexion or extension) with no initial slack. During the test, the tape tightened and stretched, allowing the head to move forward (Figures 14 and 15). In one test, the tape broke prior to the CRS impact with the door. In another test, the tape came unsecured from the seat back prior to impact. In the other 5 tests, the tape stayed secure and broke at impact of the CRS to the door. When the tape did stay secure during the run-up, the head rebounded from the maximum forward position such that head had a rearward displacement from neutral position at impact, also noted by the slack in the tape in Figure 15.

With the head taped or untaped, the ATD head flexed forward and rebounded during the 800 mm run-up from the initial staged position to impact with the foam door face. Therefore, the position of the ATD head at maximum engagement of the CRS to the door was similar for both test configurations (Figure 16).

Following the ATD head motion assessment by the contracting officer's technical representative (COTR), it was determined that all remaining tests be conducted without tape on the ATD head. The COTR indicated that similar head motion was present in the sled tests performed on an acceleration sled.

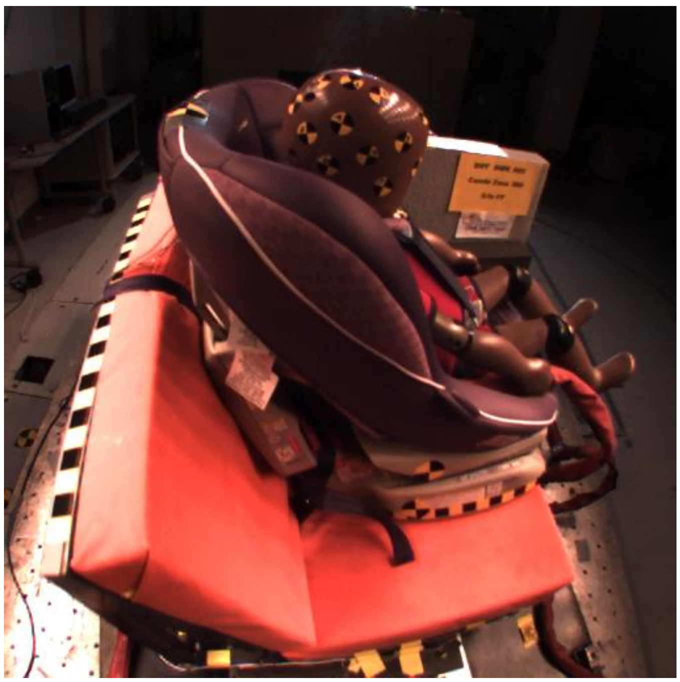

Figure 13: Inline views of Q3s left at time of impact of CRS with the door foam from Phase I testing

Figure 14: Overhead still photos from high-speed video depicting maximum forward movement of untaped and taped ATD head

Figure 15: Overhead still photos from high-speed video depicting maximum forward and rearward movement of taped ATD head

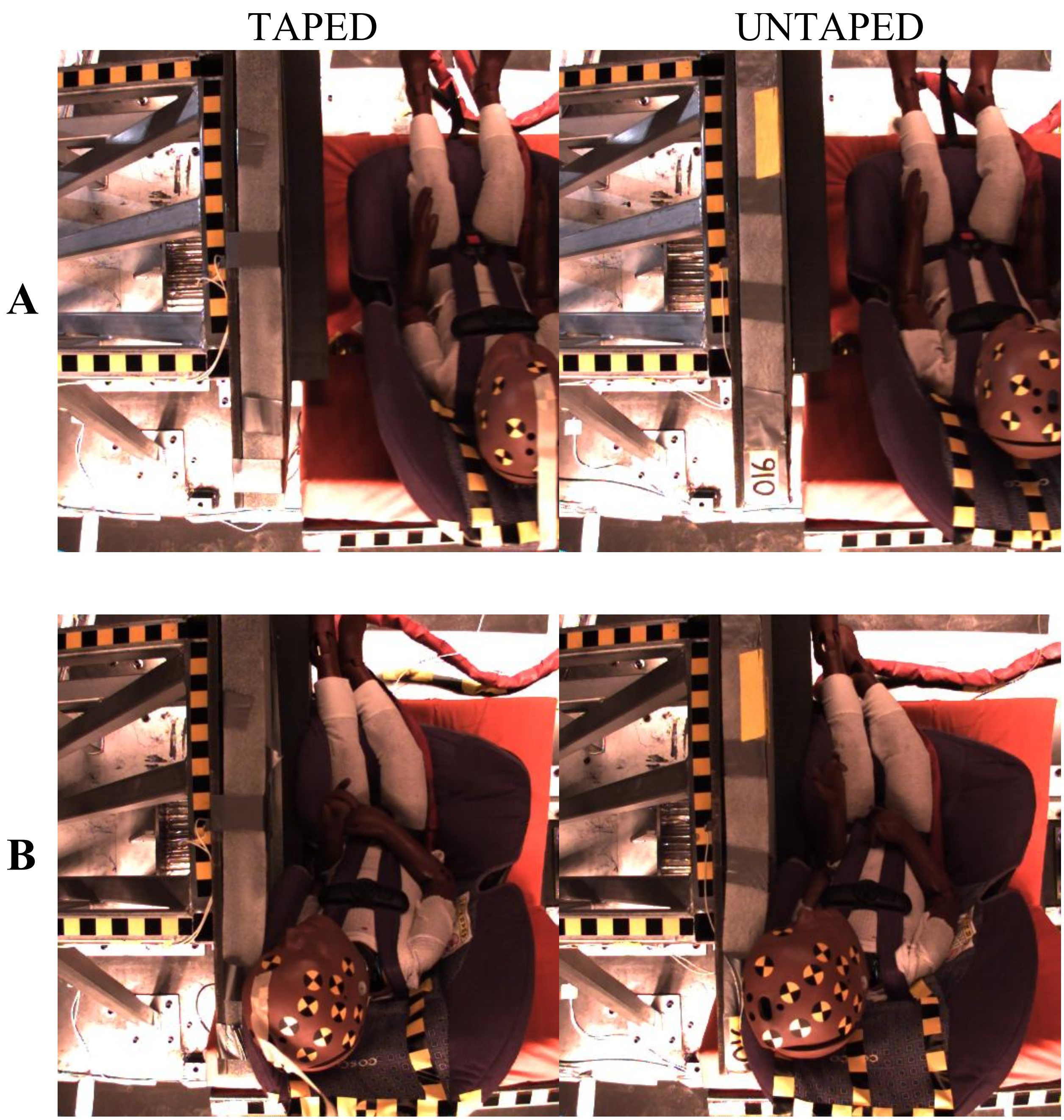

Figure 16: Overhead still photos from high-speed video depicting the taped and untaped ATD head position (A) at impact of the secondary carriage to the aluminum honeycomb and (B) at maximum engagement of the CRS to the door

4.3 Acceleration and Velocity Assessment

Seventeen Baseline I tests were conducted. Two of the tests were conducted at lower than the prescribed speeds in order to assess fixture modification feasibility and alignments. The remaining 15 tests were conducted at speeds (for the primary carriage), from a high of 33.5 kph

(20.8 mph) to a low of (18.5 mph). At the completion of the baseline series, target speed for contact of the secondary carriage to the door (test speed) of 31.3 kph (19.5 mph) was defined by the COTR for the remaining tests in the series.

Because the test speed is defined as the speed of impact of the secondary carriage to the door, the deceleration sled must target a higher speed. When the primary carriage impacts the decelerator, the secondary carriage begins to slide along the linear bearings at a 10º angle relative to the primary carriage's direction of travel. During this relative motion, the secondary carriage loses speed due to friction. In the example shown in Figure 17, there is a 0.8 mph loss of speed by the secondary carriage as it travels through the 800 mm run-up. This speed loss must be accounted for when setting the speed for the primary carriage.

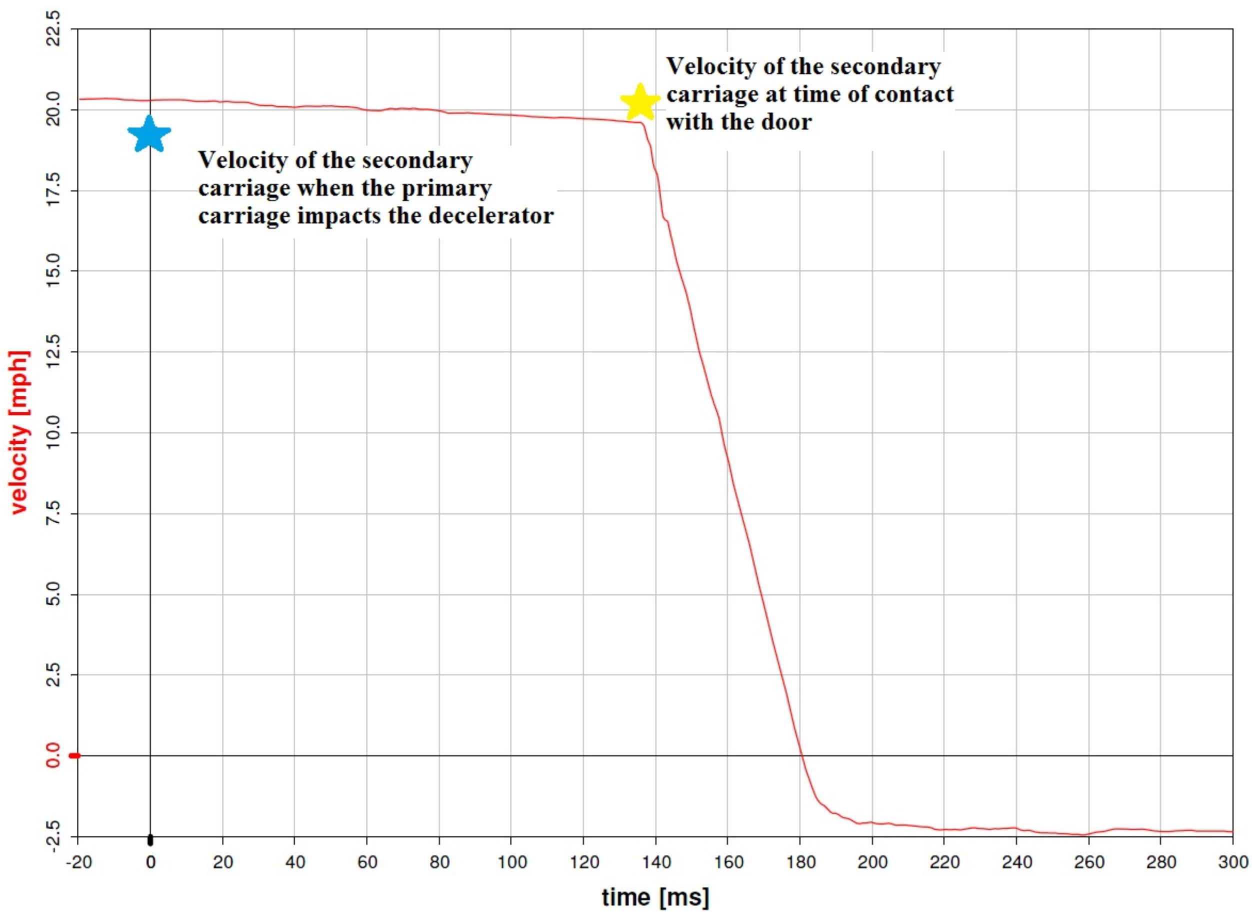

Figure 17: Velocity of the secondary carriage during a "typical" test

Four methods for determining test speed (impact speed of the secondary carriage with the door fixture) were used in the Baseline I analysis. In all cases, the speed of the secondary carriage was derived with respect to the primary carriage. The measurement devices included:

- Integration of the measured acceleration,
- "One-pass" optical sensor,
- "Multi-pass" optical sensor, and
- "Multi-pass" proximity sensor.

By standard practice, the time history of the velocity of the sled is determined from integration of acceleration with respect to time. This method uses a calibrated accelerometer output, filtered, and numerically integrated. Numerical error will be present but can be limited in the analysis. The speed at the time of impact to the door can be retrieved from the time history data.

A “one-pass” optical sensor determines the amount of time that it takes for a piece of fixed length material (gate) to pass through or past the sensor. The sensor system, in this case a GHI Systems VS200 Velocimeter, is calibrated by the manufacturer and has an output of time. The gate can be constructed of any rigid material. In this test series, a piece of 25.4 mm wide steel was used. Since the sensor uses light to determine the passing of the gate, the light source of the sensor must be shielded from ambient light to eliminate potential errors. The speed immediately prior to impact can be determined by dividing the width of the gate by the time measured from the device.

The multi-pass optical and proximity sensors calculate average velocity using an “on–off” setup to measure time over a set of 25 mm intervals (i.e., reflective tape segments, open/closed gate). The sensor itself only measures on and off (i.e., light and dark, open and closed, close and far) therefore is not calibrated with respect to a kinematic measure. The reflective tapes or gates must be precisely machined so that the software, which determines time from the sensor signal, can convert the time to velocity for each of the steps. Several factors played a role in obtaining repeatable data including ambient light, the characteristics of the “gate” machining, and the software (edge detection and sample time). Figure 18 represents an output from one of the multi-pass sensors used during this study. While the sensor was shielded from ambient light and the gates were machined using a computer numerical controlled (CNC) process, the software was not robust enough to determine “on and off” within the test tolerances at the speeds in which the sled was travelling. Since the speed should be consistently increasing or constant prior to impact with the door, it is evident from the data that the multi-pass sensor (and software) did not process the data within the tolerances needed for this testing.

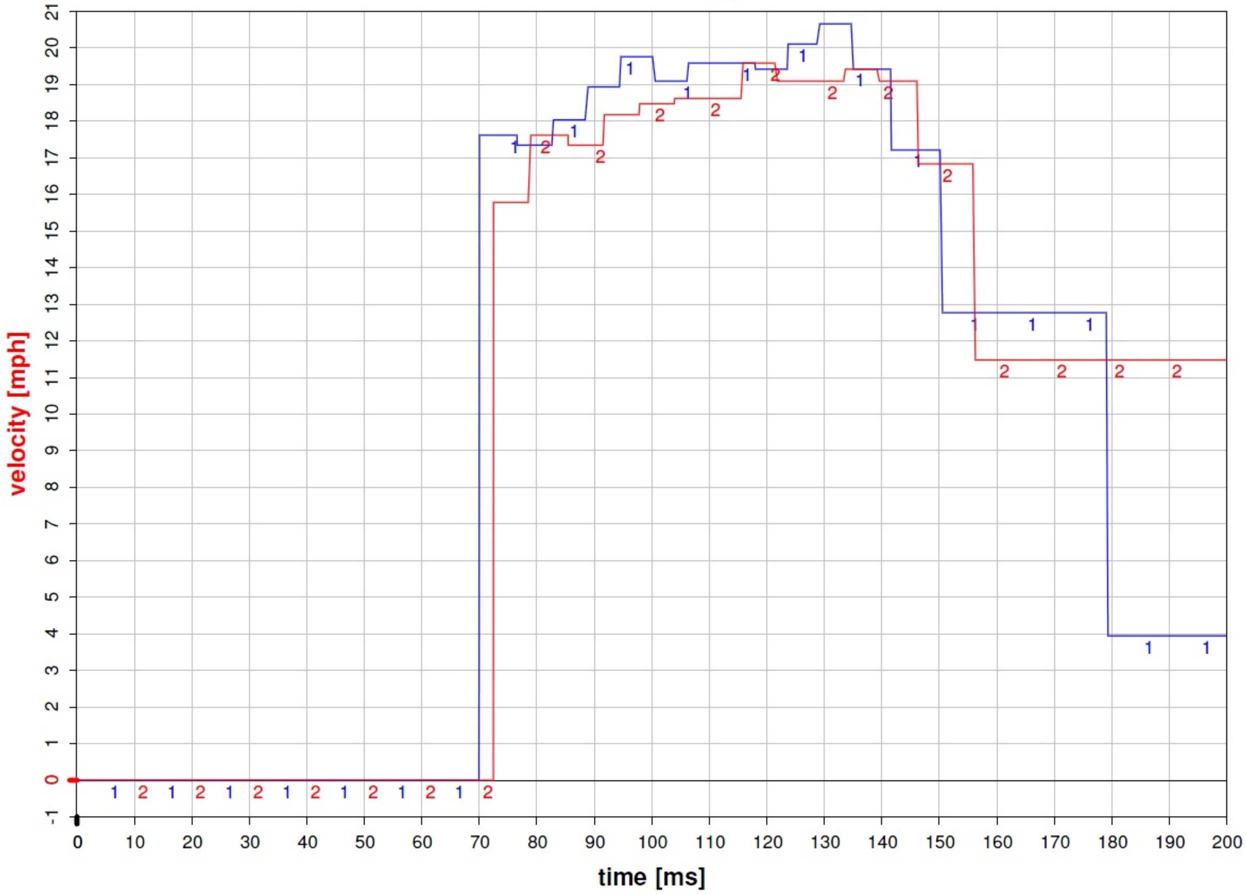

Figure 18: Velocity of the secondary carriage for two 19.0 mph tests as measured by a multi-pass proximity sensor

Upon consideration of the resulting velocity readings from various measurement devices, it was determined to use the GHI Systems VS200 Velocimeter for the child restraint testing series. It provided the most consistent secondary velocity reading among the sensors evaluated and served as a confirmation tool for assessing the secondary carriage velocity as determined with integration of the acceleration data.

4.4 Test Repeatability

Figures 19 and 20 demonstrate the repeatability of the results from Baseline I Tests 16 and 17, the final two tests prior to the first set of CRS specific tests.

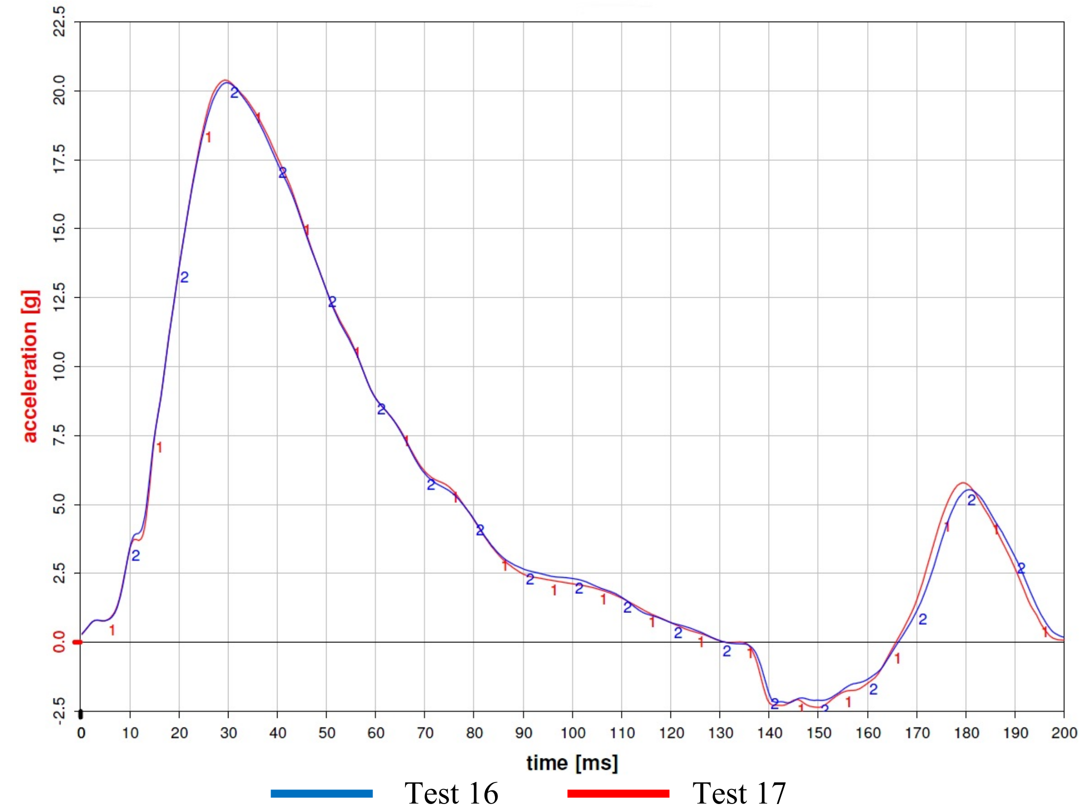

Figure 19: Primary carriage acceleration for Tests 16 and 17

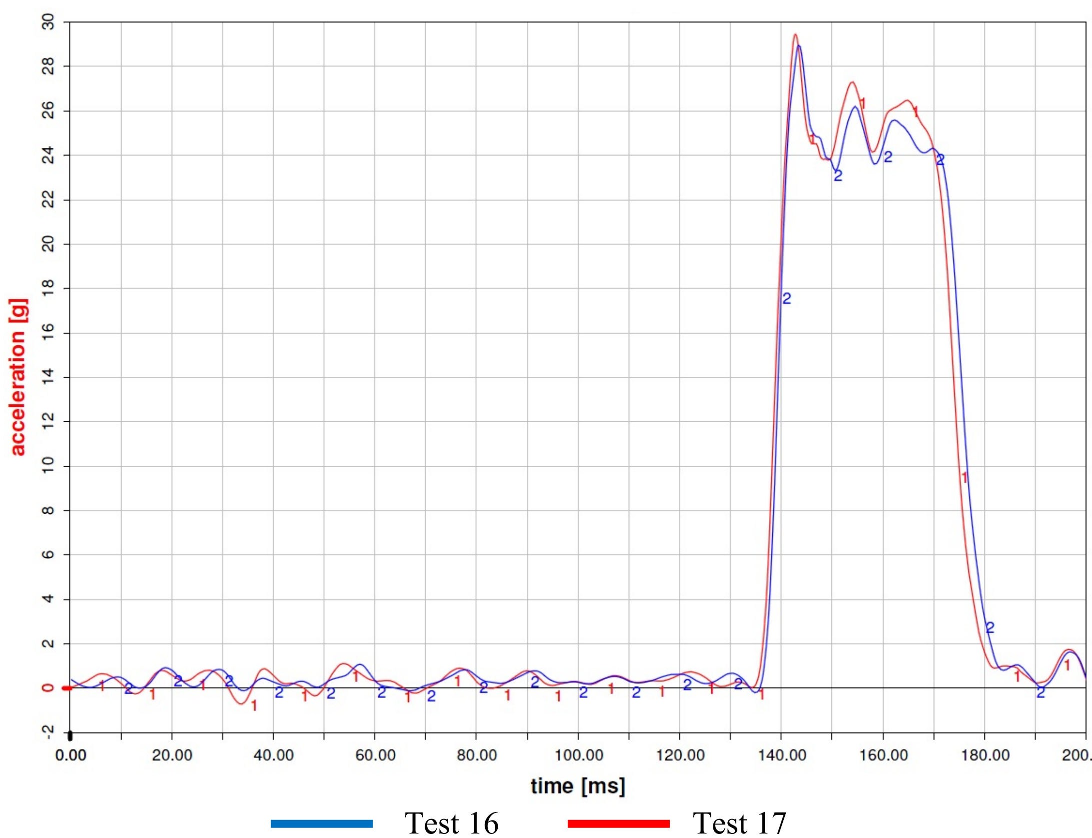

Figure 20: Secondary carriage acceleration (seat back position) for Tests 16 and 17

5.0 Performance Testing of CRS: Tests 019 to 026

Once the test parameters were determined by Baseline Testing Series I, the prescribed series of 8 side impact tests were performed on the deceleration sled. The test matrix is defined in Table 5. The tests in this series were conducted with a secondary carriage weight of 102 kg (225 lb).

Table 5: Test matrix for DOT SIDE 019 to 026[1]

Test Number	ATD	Child Restraint System (CRS)	Note
019-021	Q3s (left side)	Graco Classic Ride 50 – FF	LATCH*
022-024	Q3s (left side)	Graco Nautilus – FF	LATCH*
025-026	CRABI 12	Cosco Scenera – RF	LATCH,* lower anchors only

*Lower Anchors and Tether for Children

The tests were conducted using the procedures specified in TP-213-09 and side impact testing procedures found in Appendix B. All data were processed per SAE J211. Data acquisition and analysis was conducted using the Autolab and Eval software, respectively.

The primary and secondary carriage responses for tests DOT SIDE 019 to DOT SIDE 026 are listed in Table 6. The incoming speed of the primary carriage ranged from 19.8 mph to 20.1 mph. In all cases, the primary carriage came to rest prior to the impact with the secondary carriage. By integrating the secondary carriage seat back accelerometer data, the secondary carriage impact speeds with the aluminum honeycomb ranged from 19.4 mph to 19.7 mph. This impact range was within the critical parameter of speed of 19.5 $\pm$ 0.5 mph. Additional velocity data was collected using the GHI single pass velocity sensor. The velocity ranged from 19.7 mph to 19.9 mph. The average peak deceleration of the secondary carriage for this series of tests, in which the secondary carriage mass was 225 lb, was 27.8 g and the average amount of honeycomb crush was 125 mm.

The resulting injury values of the Q3s and CRABI12 are summarized in Table 7 and Table 8, respectively. Time histories for all ATD channels are provided in the individual test reports.

[1] These tests can be accessed through the NHTSA vehicle database at http://www-nrd.nhtsa.dot.gov/database/VSR/veh/QueryTest.aspx. The respective test numbers, 8300 to 8307, are in the vehicle database.

Table 6: Primary and secondary carriage response for tests DOT_SIDE_019 to DOT_SIDE_026

TEST NUMBER	CHILD RESTRAINT SYSTEM	ATD TYPE/ DIRECTION	RESTRAINT TYPE	PRIMARY CARRIAGE SPEED INCOMING (kph/mph)	IMPACT VELOCITY TO DOOR (kph/mph)	VELOCITY SENSOR SECONDARY CARRIAGE (kph/mph)	PEAK DECELERATION OF SEAT BACK (g)	TIME OF PEAK DECELERATION OF SEAT BACK (ms)	AMOUNT OF HONEYCOMB CRUSH (mm)
DOT_SIDE_019	Graco Classic Ride 50	Q3s left/FF	LATCH	31.9/19.8	31.4/19.5	31.7/19.7	27.8	164.0	120.0
DOT_SIDE_020	Graco Classic Ride 50	Q3s left/FF	LATCH	32.0/19.9	31.2/19.4	31.9/19.8	27.3	143.5	135.0
DOT_SIDE_021	Graco Classic Ride 50	Q3s left/FF	LATCH	32.0/19.9	31.4/19.5	31.7/19.7	27.5	144.6	125.0
DOT_SIDE_022	Graco Nautilus	Q3s left/FF	LATCH	32.0/19.9	31.4/19.5	32.0/19.9	27.0	154.8	128.0
DOT_SIDE_023	Graco Nautilus	Q3s left/FF	LATCH	31.9/19.8	31.4/19.5	31.7/19.7	27.3	155.7	127.0
DOT_SIDE_024	Graco Nautilus	Q3s left/FF	LATCH	31.9/19.8	31.4/19.5	31.7/19.7	29.5	155.6	115.0
DOT_SIDE_025	Cosco Scenera	CRABI12 RF	LATCH w/o tether	32.2/20.0	31.4/19.5	31.7/19.7	29.2	154.7	121.0
DOT_SIDE_026	Cosco Scenera	CRABI12 RF	LATCH w/o tether	32.3/20.1	31.7/19.7	31.9/19.8	26.4	154.6	127.0

Table 7: ATD response for tests DOT_SIDE_019 to DOT_SIDE_024

TEST NUMBER	**CHILD RESTRAINT SYSTEM**	**ATD TYPE/ DIRECTION**	**IMPACT SPEED TO DOOR (kph/mph)**	**HEAD CONTACT**	**MAX RESULTANT HEAD ACCEL (g)**	**HIC 15/36**	**MAX SHOUL DER DISP (mm)**	**MAX IR-TRACC DISP (mm)**	**MAX RESULTANT UPPER SPINE ACCEL (g)**	**MAX PUBIC FORCE (N)**	**MAX RESULTANT PELVIC ACCEL (g)**
DOT_SIDE_019	Graco Classic Ride 50	Q3s FF	31.4/19.5	yes	105.8	781/781	23.9	23.7	85.6	147.1	105.9
DOT_SIDE_020	Graco Classic Ride 50	Q3s FF	31.2/19.4	yes	99.8	734/734	23.1	26.6	83.7	181.1	118.0
DOT_SIDE_021	Graco Classic Ride 50	Q3s FF	31.4/19.5	yes	97.0	698/698	22.5	27.7	88.9	150.4	113.2
DOT_SIDE_022	Graco Nautilus	Q3s FF	31.4/19.5	no	78.2	559/559	17.9	20.2	111.5	110.2	133.4
DOT_SIDE_023	Graco Nautilus	Q3s FF	31.4/19.5	no	81.5	593/593	17.0	14.8	channel fault	466.8	132.8
DOT_SIDE_024	Graco Nautilus	Q3s FF	31.4/19.5	no	89.3	625/625	20.2	20.5	channel fault	331.2	144.7

Table 8: ATD response for tests DOT_SIDE_025 and DOT_SIDE_026

TEST NUMBER	**CHILD RESTRAINT SYSTEM**	**ATD TYPE/ DIRECTION**	**IMPACT SPEED TO DOOR (kph/mph)**	**HEAD CONTACT**	**MAX RESULTANT HEAD ACCEL (g)**	**HIC 15**	**HIC 36**	**MAX RESULTANT CHEST ACCEL (g)**	**MAX RESULTANT PELVIC ACCEL (g)**
DOT_SIDE_025	Cosco Scenera	CRABI12 RF	31.4/19.5	no	98.5	618	618	94.5	95.3
DOT_SIDE_026	Cosco Scenera	CRABI12 RF	31.7/19.7	no	87.6	597	597	127.2	108.8

6.0 Baseline Testing: Part II

The objective of the Baseline II test series was to assess the secondary carriage acceleration and relative velocity time history with varying secondary carriage weight and aluminum honeycomb volume. The spacing of the impact planes, honeycomb-to-secondary carriage and CRS-to-door, was also evaluated.

6.1 Calculation of relative velocity

While the Baseline I test series focused on the instantaneous impact speed of the secondary carriage to the door, the Baseline II series introduced the study of the speed of the secondary carriage with respect to the primary carriage perpendicular to the door, for the complete test event (Figure 21). The details of the relative velocity calculation are outlined in Appendix A.

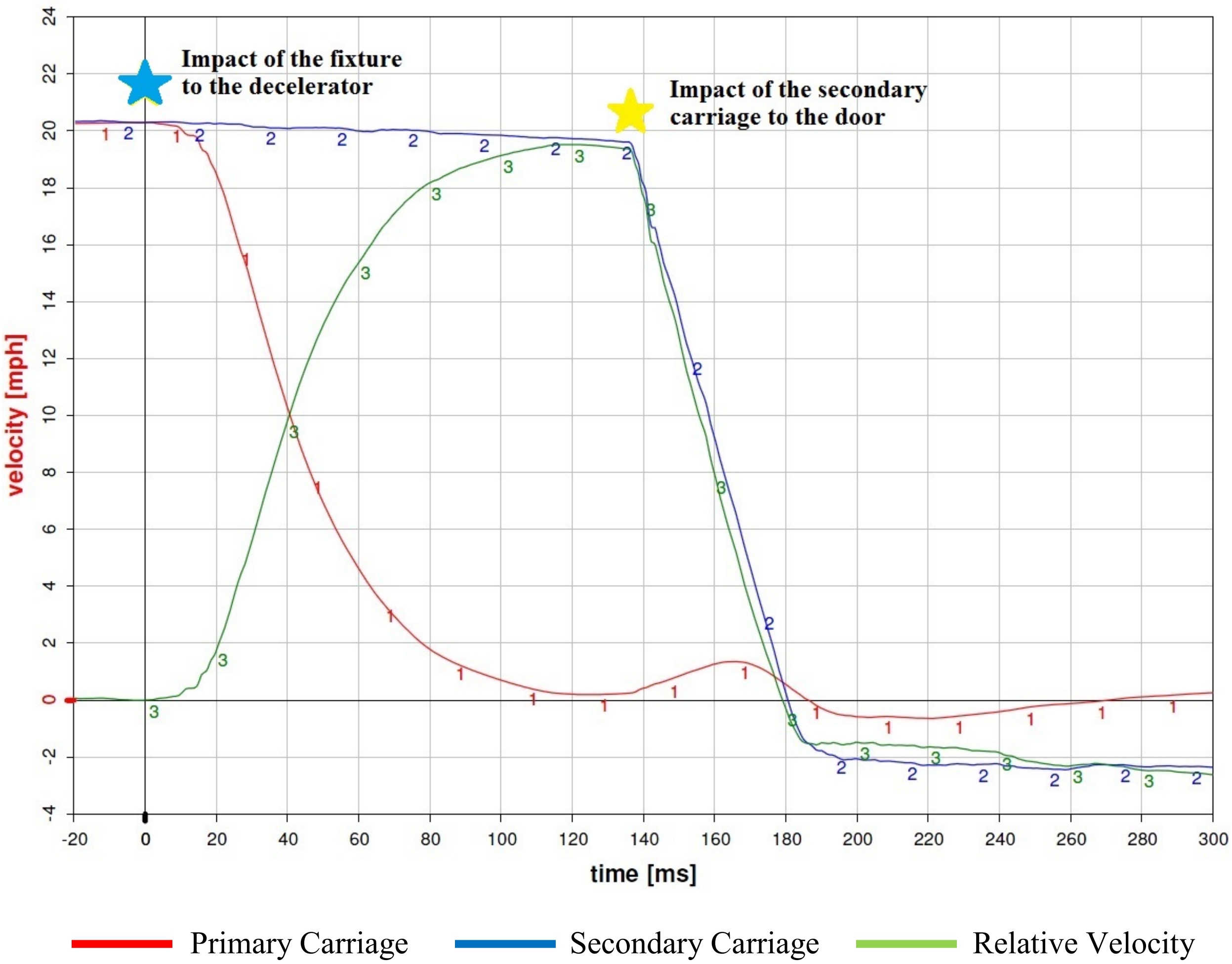

Figure 21: Absolute velocities of the primary and secondary carriages with the corresponding relative velocity

6.2 Variation of speed

In Baseline Series I, the instantaneous speed of impact of the secondary carriage to the door was assessed. In Baseline Series II, the relative velocity between the two carriages was studied. Using the test data from Baseline Series I, a determination of the effect of speed on the acceleration and relative velocities was conducted.

Figure 22 shows the comparison of secondary carriage acceleration for three tests of varying speed. Each test was conducted as part of Baseline I; therefore the secondary carriage weight is 225 lb. With the reduction of speed, the area under the acceleration versus time curve must decrease since the velocity is the integral of acceleration with respect to time. The reduction in the area can occur in two ways (or a combination of the two): a reduction in the amplitude of the acceleration or a reduction in the duration. When the only change to the test is speed, the acceleration time history depicts a combination of both the reduction of acceleration amplitude and time duration.

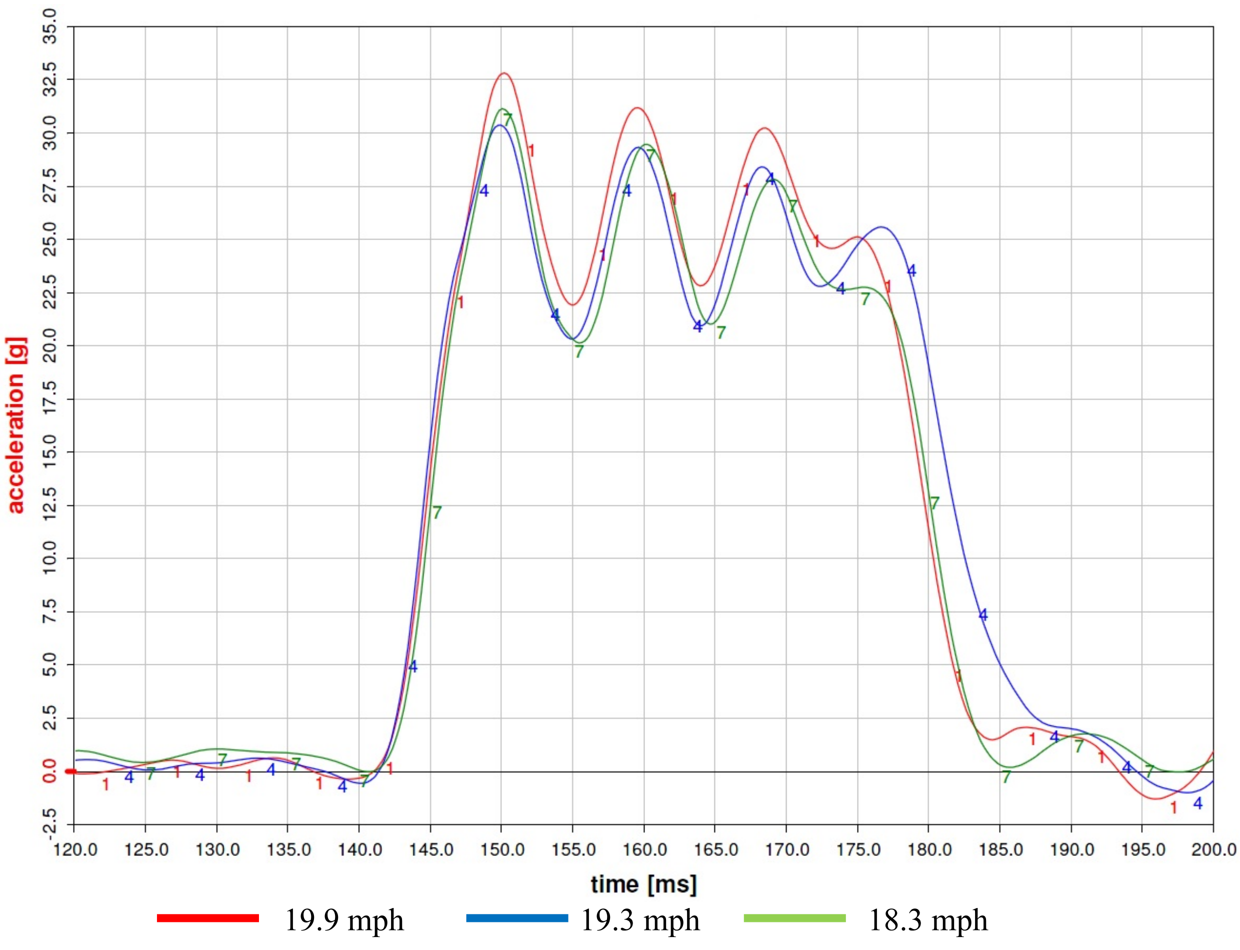

Figure 22: Acceleration time histories for side impact tests conducted at varying speeds (tests conducted with the 225 lb secondary carriage)

When assessing the corresponding relative velocities for the tests with speed variation (Figure 23), several factors can be viewed. One aspect is that with a greater speed, the secondary carriage impacts the primary carriage in a shorter time with respect to time zero (as defined by the impact of the primary carriage to the decelerator). Therefore, to be able to compare from test-to-test, the secondary carriage relative velocity during contact with the primary carriage door, a trigger switch was added to the testing for CRS testing 027 to 038. The trigger allows for the alignment of time of impact to the door (Figure 24). Since the switch was not used in the first series of tests, the data in Figure 24 is time shifted (from time zero) by aligning the inflection points on the velocity curves. The trigger allows for a more precise way of aligning the data. With the relative velocities aligned, it can be noted that the rate of change of the velocity is comparable between the three tests.

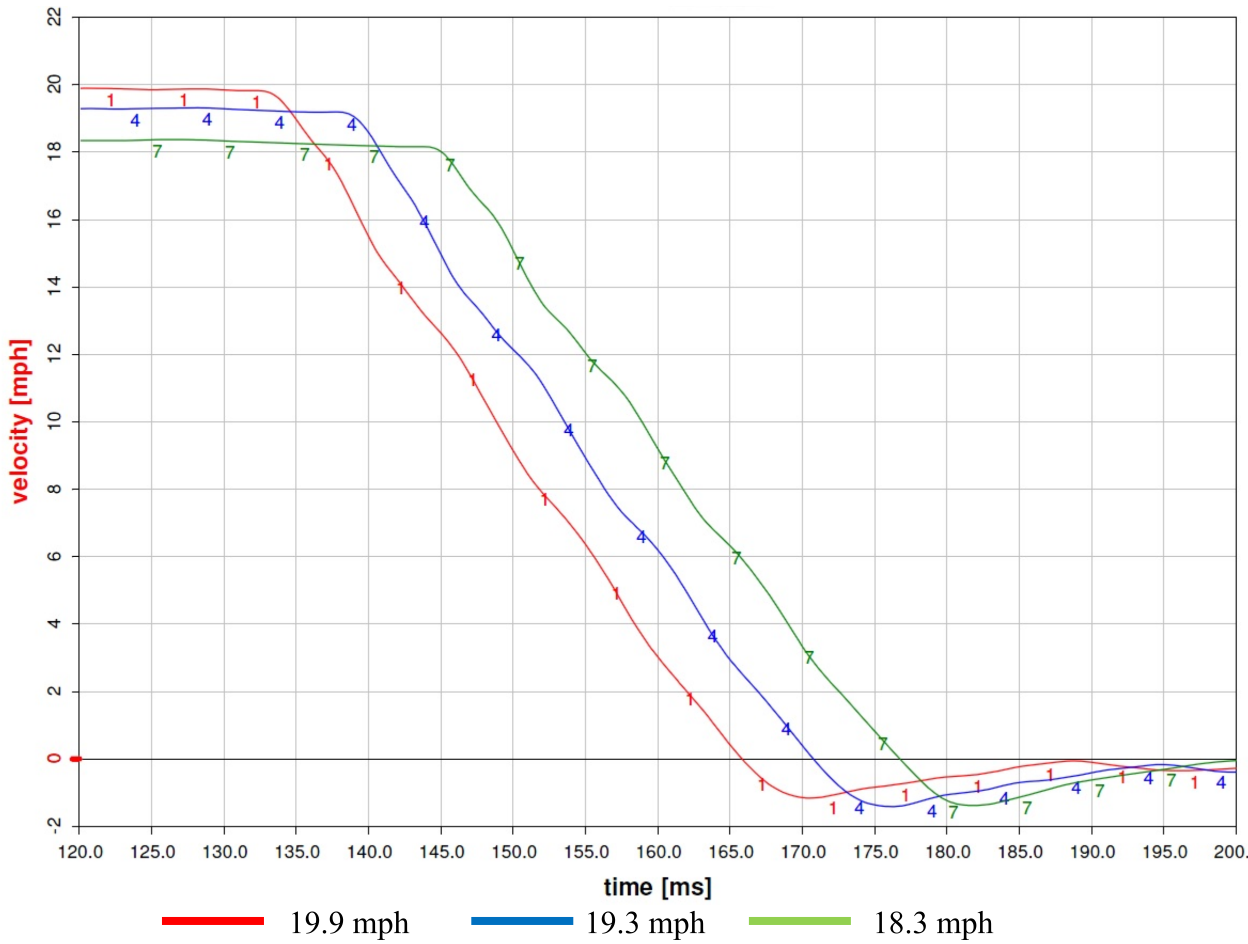

Figure 23: Relative velocity time histories for side impact tests conducted at varying speeds (tests conducted with the 225 lb secondary carriage)

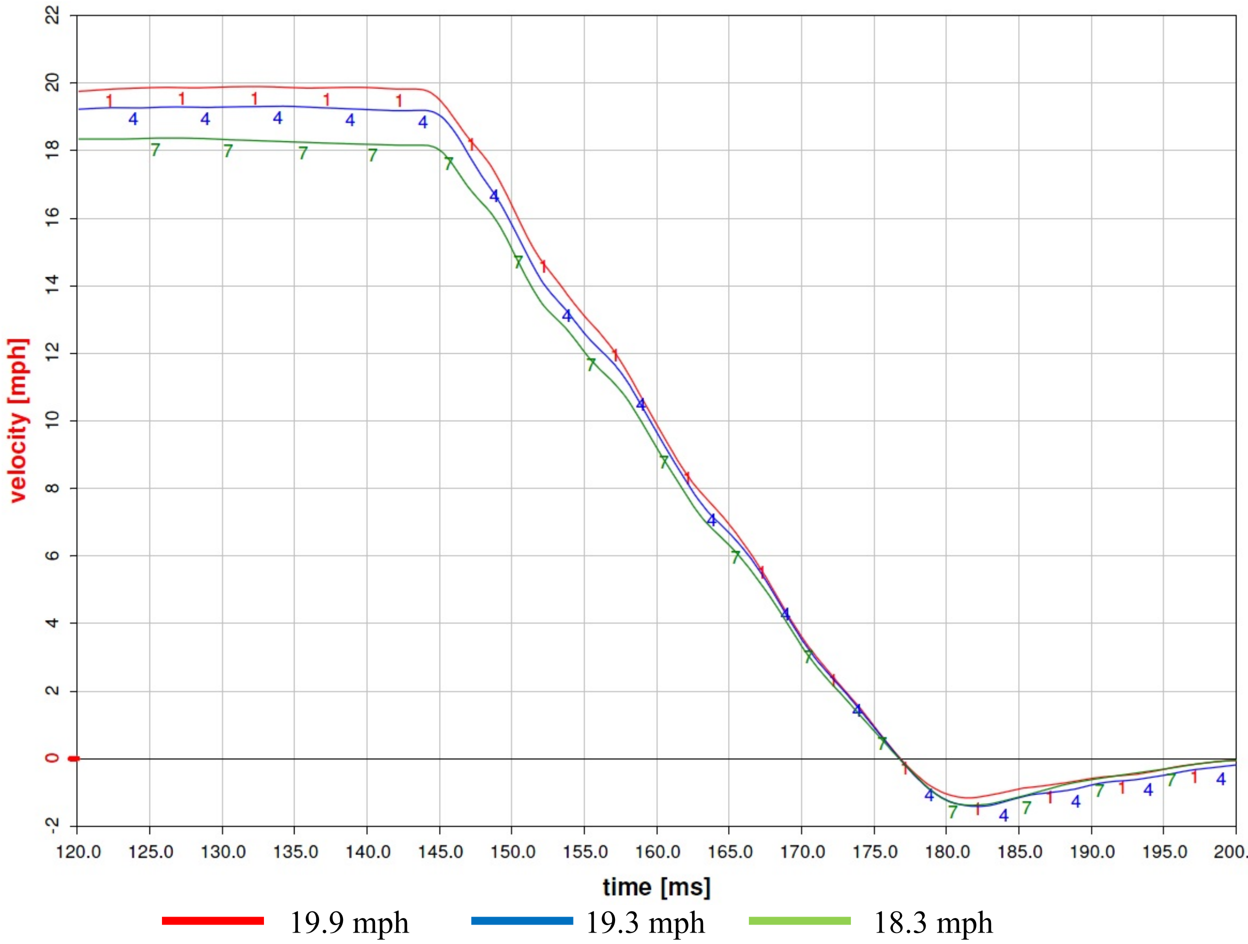

Figure 24: Relative velocity time histories for side impact tests conducted at varying speeds, time shifted to align time-of-impact with the door (tests conducted with the 225 lb secondary carriage)

6.3 Variation of secondary carriage weight

The weight of the secondary carriage was altered from 225 lb, to 256 lb, to 279 lb. The weight variation was achieved by adding/removing plate steel to the underside of the secondary carriage bench seat. All tests were conducted with an impact speed of the secondary carriage to the primary carriage of 19.5 ± 0.3 mph. It was determined that as the weight of the carriage increased, the peak acceleration decreased and the duration of the pulse increased (Figure 25). The 256 lb carriage fell within the prescribed acceleration – time corridor for all time (Figure 26). The change in the weight also had an effect on the relative velocity (Figure 27). All the tests were conducted with a Cosco Scenera CRS and the HIII 3 YO ATD attached to the secondary carriage bench with LATCH. The combined weight of the test pieces (CRS and ATD) was 43.5 lbs.

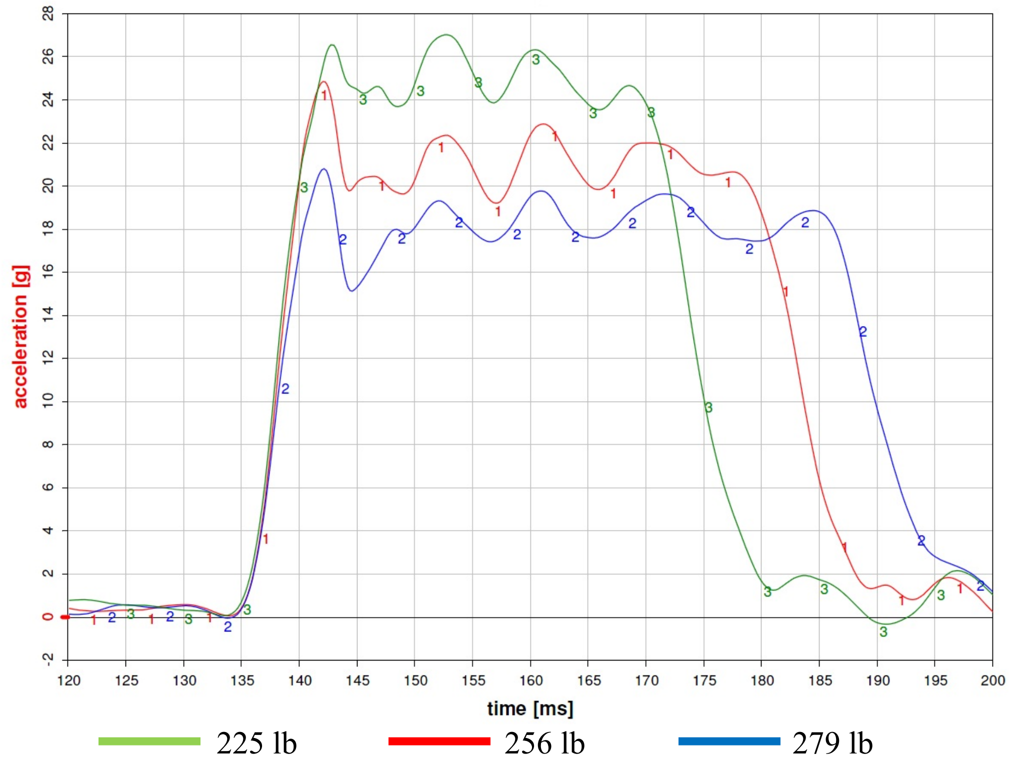

Figure 25: Acceleration of secondary carriage for three different weights

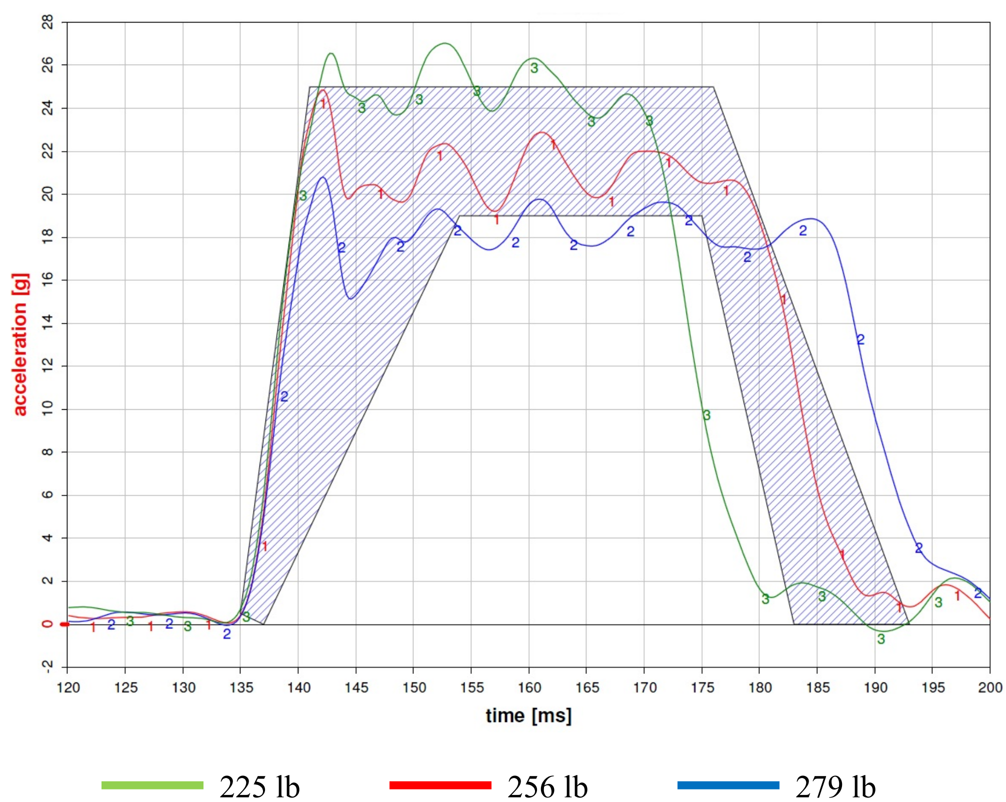

Figure 26: Acceleration of secondary carriage (with corridor) for three different weights

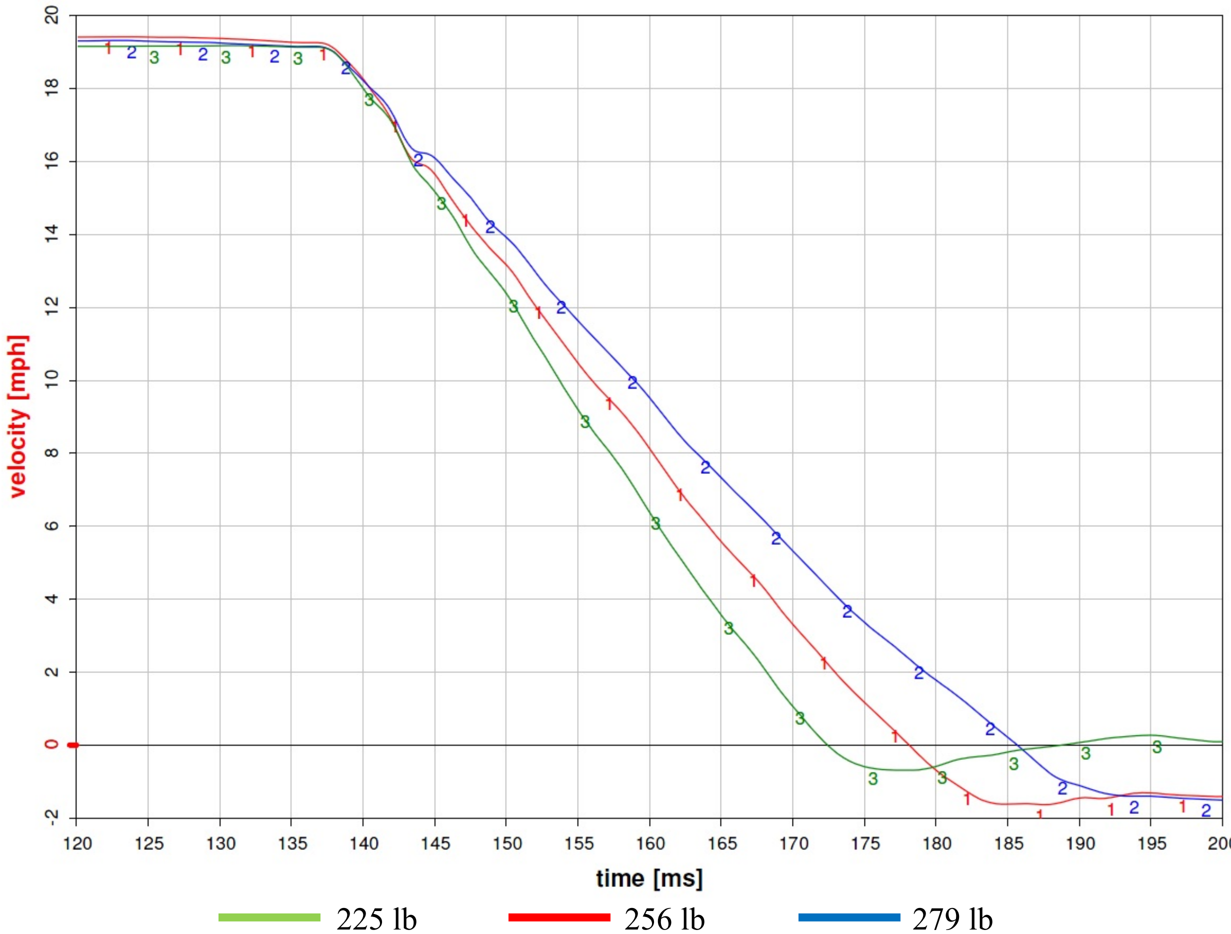

Figure 27: Relative velocity of secondary carriage for three different weights

While the weight of the secondary carriage affected the acceleration and velocity time histories, altering the test weight of the pieces on the bench (includes child restraint and dummy), did not. A 19.5 mph test was conducted on the 256 lb carriage with no test pieces (no child restraint or dummy), therefore reducing the payload by 43.5 lb. When comparing the acceleration time histories for the tests conducted with and without the test pieces, the pulses for both tests are comparable (Figure 28). A change in the pulse was not evident as seen when the carriage itself was reduced by 31 lb. This can be attributed to the fact that the CRS/ATD is not solidly attached to the secondary carriage but is affixed to the carriage with seatbelt webbing and loads the test fixture to impact with the door.

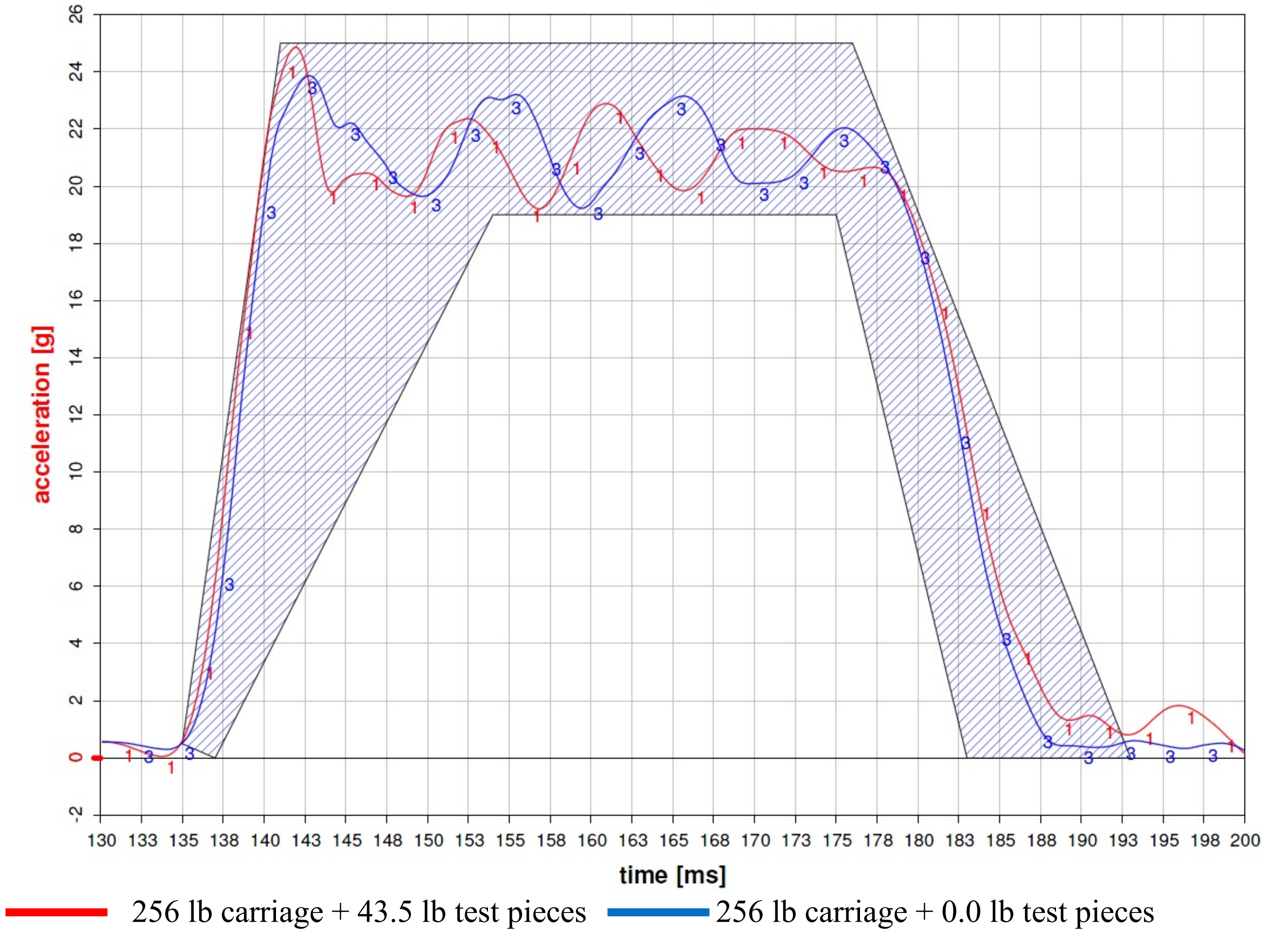

Figure 28: Acceleration (with corridor) for tests conducted with and without test pieces

6.4 Variation of aluminum honeycomb volume

To assess the sensitivity of the secondary carriage kinematics to a change in the aluminum honeycomb volume, a test was conducted in which the standard honeycomb piece was replaced with an experimental piece that had a greater impact area by 1 inch in width and length. The depth of the piece was consistent since it was cut from the same sheet of aluminum honeycomb PAMG-XR1 5052 from Plascore. Therefore, the standard volume of 810 in^3 was increased by 29% to 1044 in^3.

All tests were conducted with an impact speed of the secondary carriage to the primary carriage of 19.5 $\pm$ 0.2 mph. While the tests conducted with the standard honeycomb volume had comparable acceleration (Figure 29) and relative velocity (Figure 30) profiles, the test with greater honeycomb volume was unique. The peak acceleration was greater and the time duration shorter when a greater amount of material was available. Also, the rate of change of the velocity was greater for the larger honeycomb test piece.

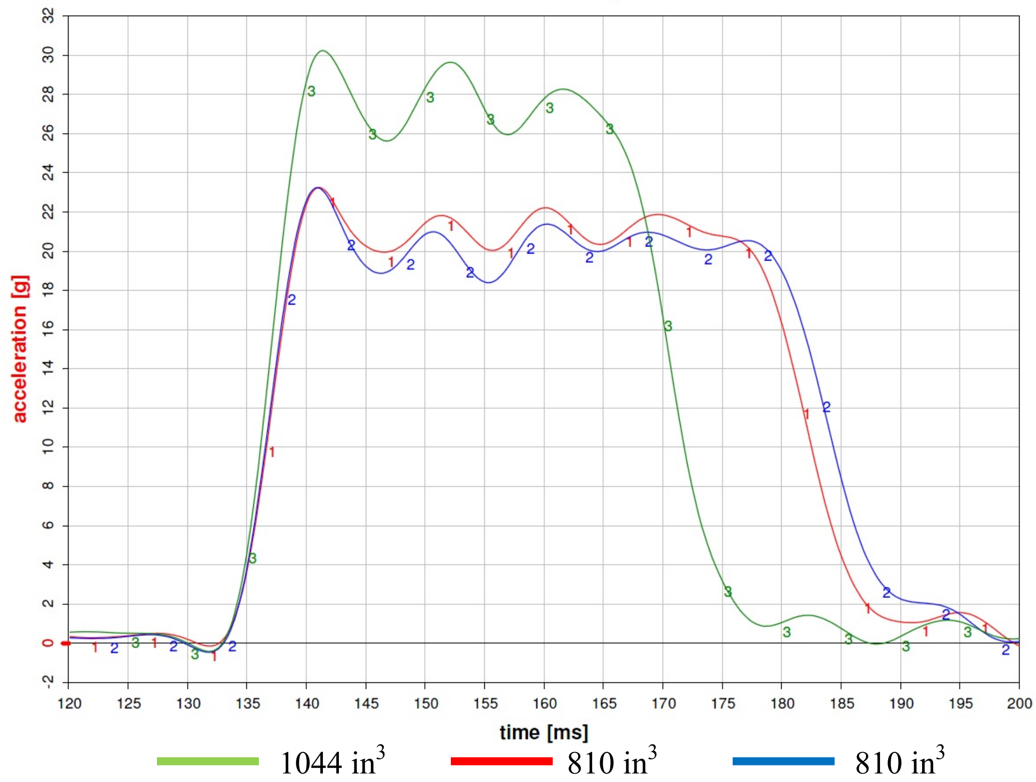

Figure 29: Acceleration of the secondary carriage for varied aluminum honeycomb volume

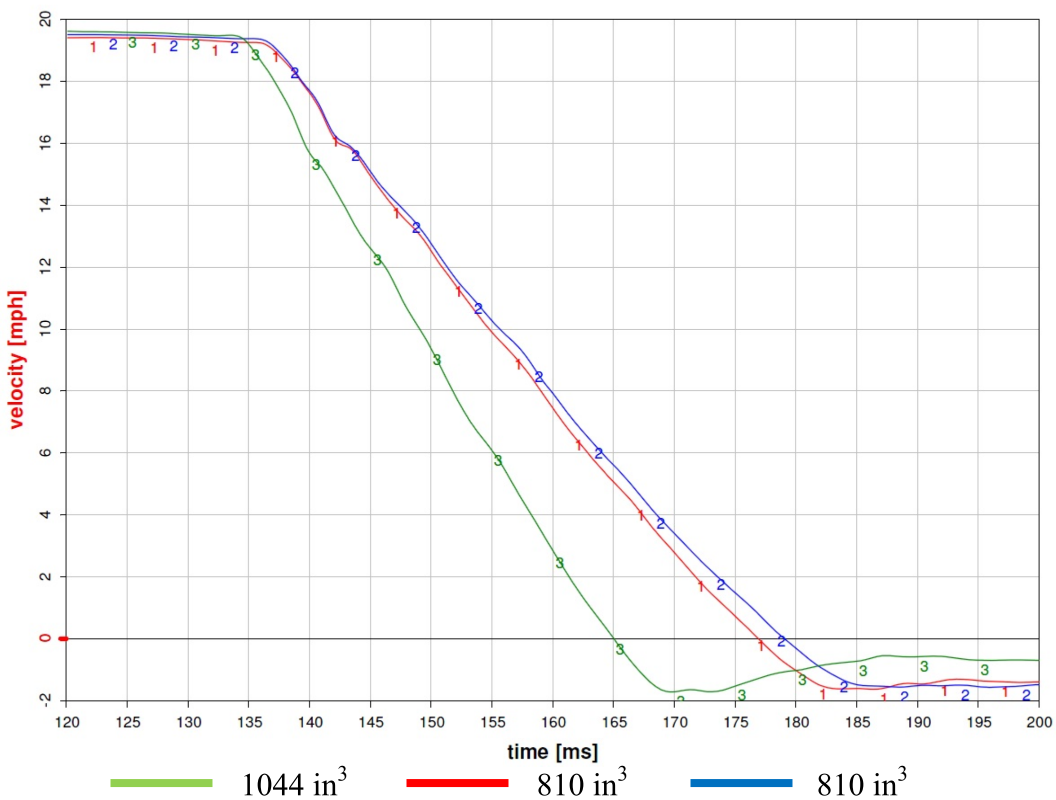

Figure 30: Relative velocity of the secondary carriage for varied aluminum honeycomb volume

6.5 Impact plane evaluation

The fixture design calls for permanent spacing for the plane of the door face to the plane of the honeycomb block at 42 mm (Figure 31). With this setup, the impact of the honeycomb-to-secondary carriage and the door-to-CRS can occur at different times, depending on the width of the CRS. One test was conducted with a Cosco Scenera and a HIII 3 YO, where the alignment of the planes was varied such that the honeycomb struck the secondary carriage and the door struck the CRS simultaneously. Taking into account the width and placement of the CRS, concurrent impact was achieved by moving the honeycomb block rearward 40 mm (1.6 in) creating 82 mm (3.2 in) of spacing from the plane of the door face to the plane of the honeycomb block (Figure 31). Therefore, when the planes were not aligned, the aluminum honeycomb block crushed 40 mm (1.6 in) prior to impact of the door to the CRS, depicted by the gap labeled in Figure 32. Altering the impact plane alignment had a nominal effect on the acceleration time history for the secondary carriage (Figure 33).

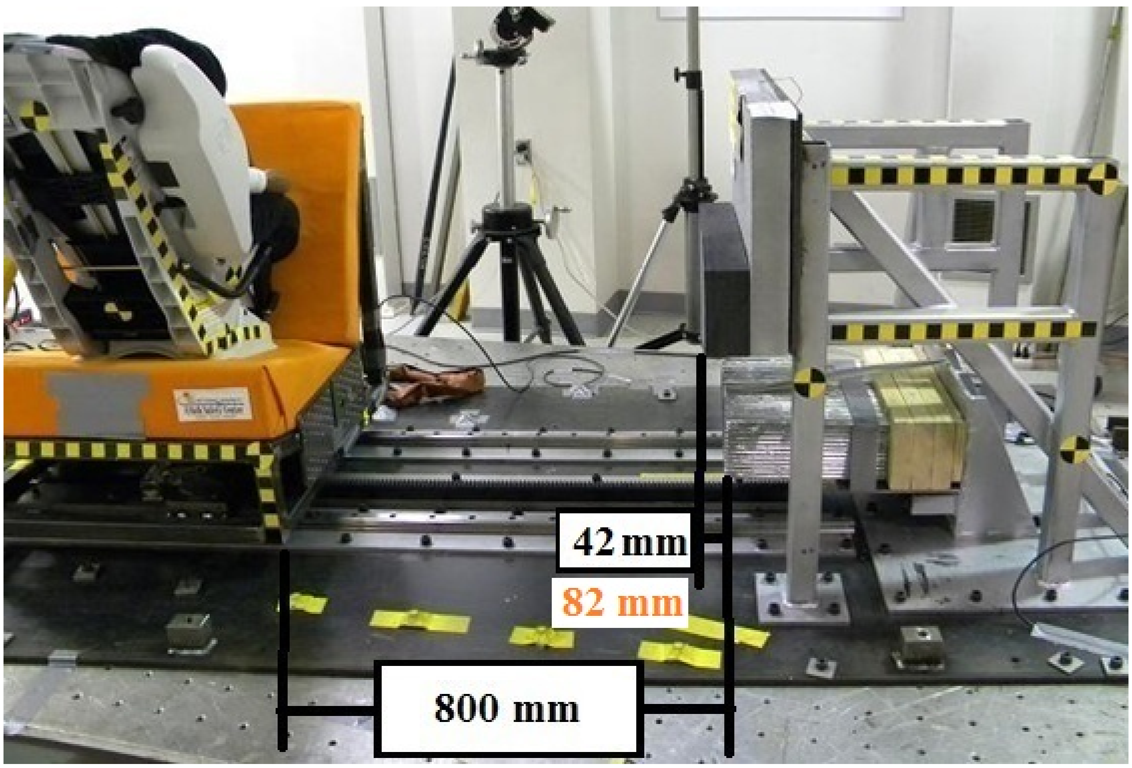

Figure 31: Standard (42 mm) and varied (82 mm) alignment of the honeycomb face from the plane of the door face

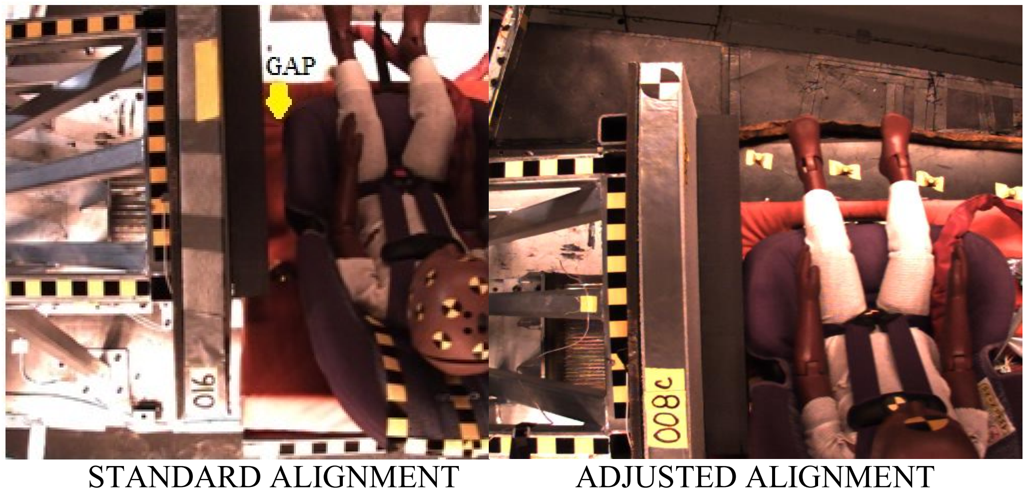

Figure 32: Overhead view of CRS-to-door interface at impact with the aluminum honeycomb

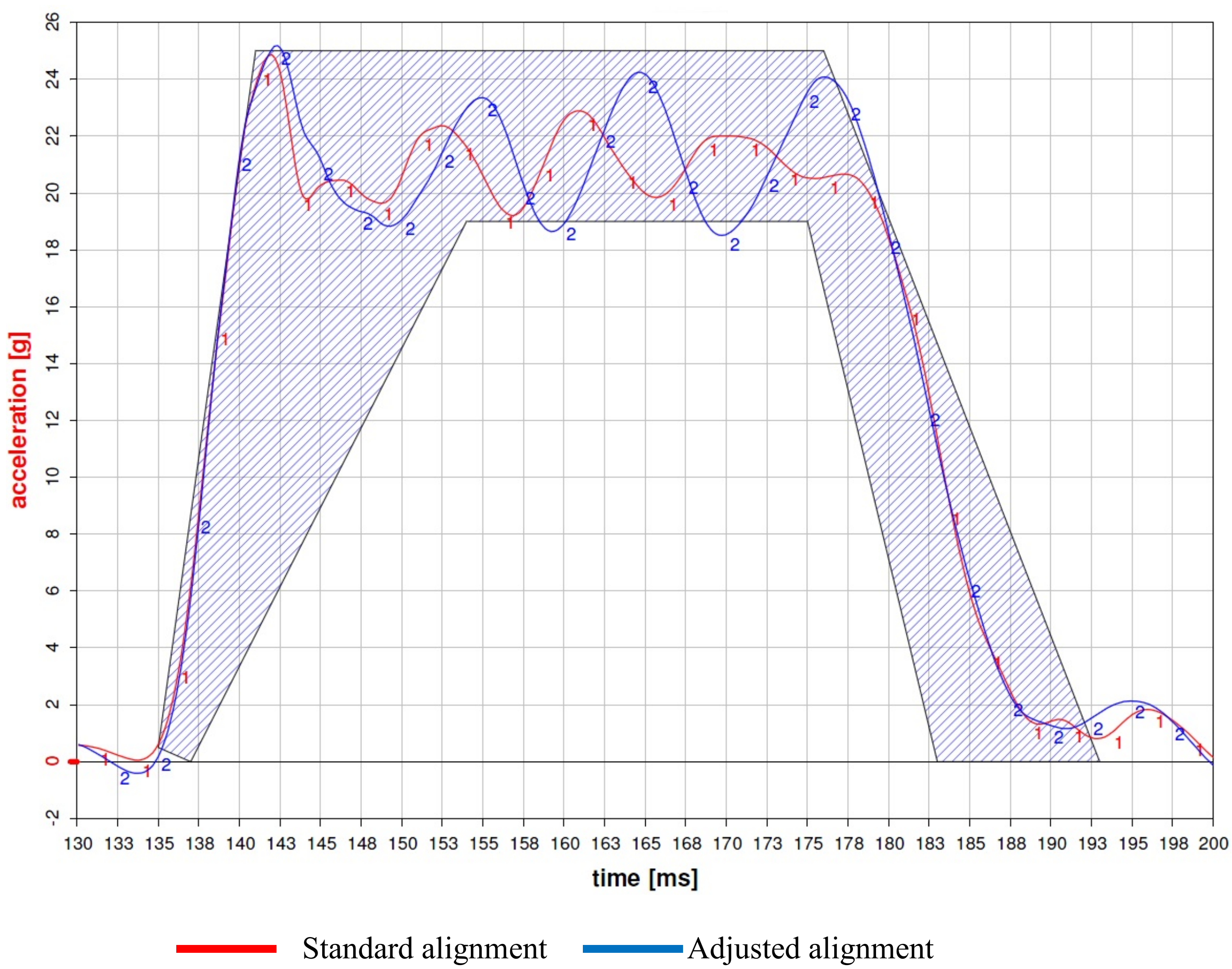

Figure 33: Acceleration of the secondary carriage (with corridor) for tests with two different impact plane alignments

Even though the impact timing sequence did not affect the acceleration time history, the timing does alter the impact environment for the CRS. The initial 40 mm of crush slowed the secondary carriage such that the speed of impact of the CRS to the door was different between the two scenarios. With the impact planes aligned, the CRS was struck at the same speed as the honeycomb, in this test, 19.2 mph. When the honeycomb was set at the fixed position of 42 mm from the plane of the door, the door struck the CRS 5 msec after impact with the honeycomb resulting in a reduced impact speed of 16.8 mph (Figure 34). Therefore, with a 12.5-percent reduced impact speed, the fixed position CRS had a 23-percent reduction in impact energy.

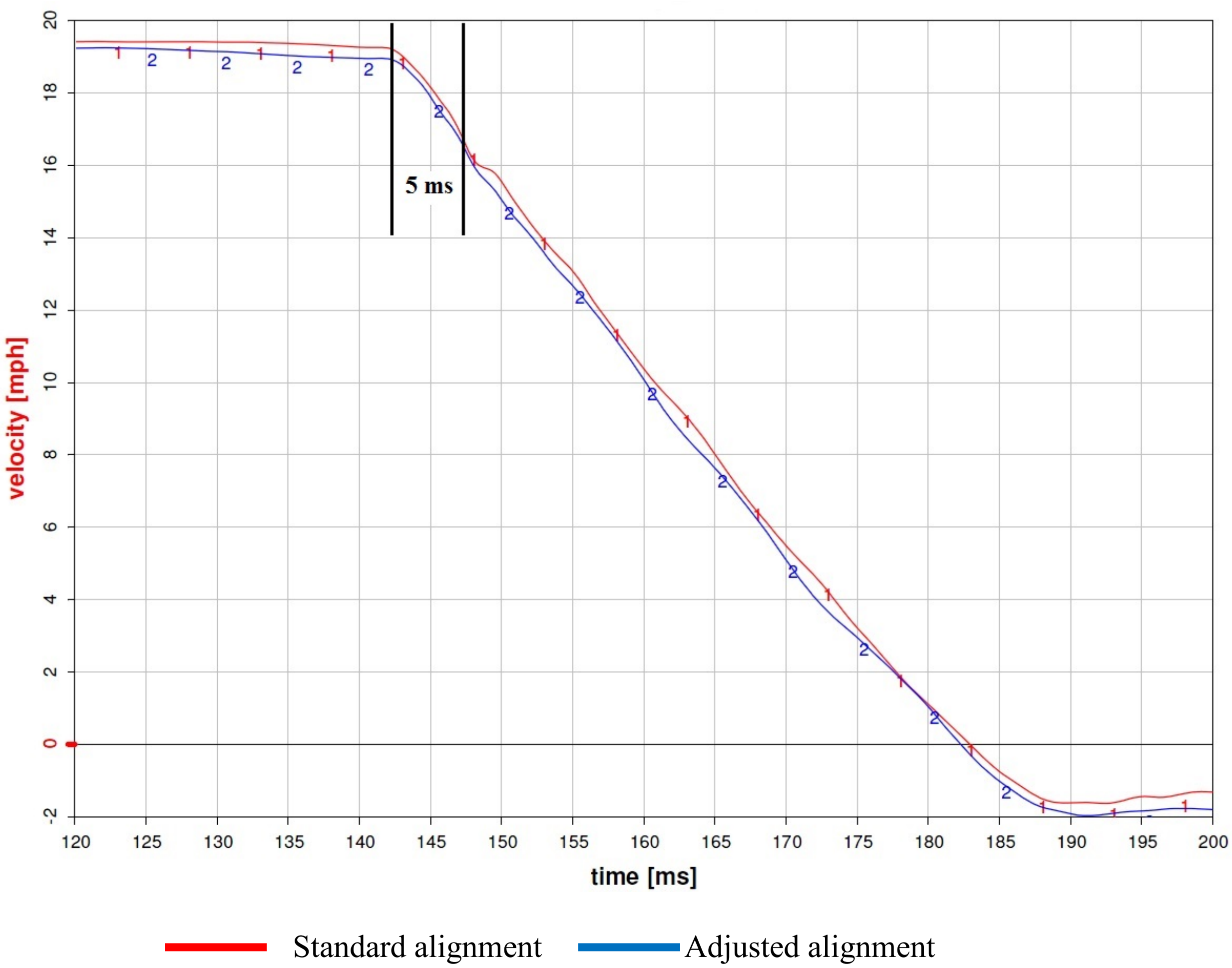

Figure 34: Relative velocity of the secondary carriage for tests with two different impact plane alignments

7.0 Performance Testing of CRS: Tests 027 to 038

Once the test parameters were determined by Baseline Testing Series II, the prescribed series of twelve (12) side impact tests were performed on the deceleration sled. The test matrix is defined in Table 9. The tests in this series were conducted with a secondary carriage weight of 116 kg (256 lb).

Table 9: Test matrix for DOT SIDE 027 to 038[2]

Test Number	ATD	Child Restraint System (CRS)	Note
027-028	Q3s (left side)	Graco Classic Ride 50 – FF	LATCH*
029-030	CRABI 12	Combi Shuttle – RF	LATCH*, lower anchors only
031-033	CRABI 12	Evenflo Discovery 5 – RF	LATCH*, lower anchors only
034-035	Q3s (right side)	Graco Classic Ride 50 – RF	LATCH*, lower anchors only
036-037	Q3s (right side)	Cosco Scenera – RF	LATCH*, lower anchors only
038	Q3s (left side)	Combi Zeus 360	LATCH*

*Lower Anchors and Tether for Children

The tests were conducted using the procedures specified in TP-213-09 and side impact testing procedures found in Appendix B. All data were processed per SAE J211. Data acquisition and analysis was conducted using the Autolab and Eval software, respectively.

The primary and secondary carriage responses for tests DOT SIDE 027 to DOT SIDE 038 are listed in Table 10. The incoming speed of the primary carriage ranged from 20.3 mph to 20.8 mph. In all cases, the primary carriage came to rest prior to the impact with the secondary carriage. By integrating the secondary carriage seat back accelerometer data and determining the relative velocity of the secondary carriage perpendicular to the door surface (along the 10^o angle), the secondary carriage impact speeds at time of contact with the aluminum honeycomb ranged from 19.3 mph to 19.7 mph. This impact range was within the critical parameter of speed of 19.5 $\pm$ 0.5 mph. Additional velocity data was collected using the GHI single pass velocity sensor. The velocity ranged from 19.7 mph to 20.2 mph. The average peak deceleration of the secondary carriage for this series of tests in which the secondary carriage mass was 256 lb, was 23.4 g and the average amount of honeycomb crush was 167 mm.

---

[2] These tests can be accessed through the NHTSA vehicle database at http://www-nrd.nhtsa.dot.gov/database/VSR/veh/QueryTest.aspx. The respective test numbers, 8331 to 8342, are in the vehicle database.

The resulting injury values of the Q3s (Table 11 and Table 13) and CRABI12 (Table 12) summarize the ATD performance. Time histories for all ATD channels are provided in the individual test reports.

Table 10: Primary and secondary carriage response for tests DOT_SIDE_027 to DOT_SIDE_038

TEST NUMBER	CHILD RESTRAINT SYSTEM	ATD TYPE/ DIRECTION	RESTRAINT TYPE	PRIMARY CARRIAGE SPEED INCOMING (kph/mph)	RELATIVE SPEED PERPENDICULAR TO DOOR AT IMPACT(kph/mph)	VELOCITY SENSOR SECONDARY CARRIAGE (kph/mph)	PEAK DECEL OF SEAT BACK (g)	TIME OF PEAK DECEL OF SEAT BACK (ms)	AMOUNT OF HONEY-COMB CRUSH (mm)
DOT_SIDE_027	Graco Classic Ride 50	Q3s left/FF	LATCH	33.0/20.5	31.4/19.5	31.7/19.7	22.8	160.0	165.0
DOT_SIDE_028	Graco Classic Ride 50	Q3s left/FF	LATCH	33.2/20.6	31.4/19.5	32.0/19.9	23.4	158.3	171.0
DOT_SIDE_029	Combi Shuttle	CRABI12 RF	LATCH w/o tether	33.2/20.6	31.4/19.5	32.0/19.9	24.2	167.2	165.0
DOT_SIDE_030	Combi Shuttle	CRABI12 RF	LATCH w/o tether	33.3/20.7	31.5/19.6	32.2/20.0	23.4	165.2	169.0
DOT_SIDE_031	Evenflo Discovery 5	CRABI12 RF	LATCH w/o tether	33.5/20.8	31.7/19.7	32.5/20.2	25.5	147.9	154.0
DOT_SIDE_032	Evenflo Discovery 5	CRABI12 RF	LATCH w/o tether	33.5/20.8	31.7/19.7	32.5/20.2	22.6	157.6	170.0
DOT_SIDE_033	Evenflo Discovery 5	CRABI12 RF	LATCH w/o tether	33.3/20.7	31.5/19.6	32.3/20.1	23.9	158.7	168.0
DOT_SIDE_034	Graco Classic Ride 50	Q3s right/RF	LATCH w/o tether	33.2/20.6	31.4/19.5	32.0/19.9	22.8	159.1	166.0
DOT_SIDE_035	Graco Classic Ride 50	Q3s right/RF	LATCH w/o tether	33.0/20.5	31.2/19.4	31.9/19.8	23.3	159.9	181.0
DOT_SIDE_036	Cosco Scenera	Q3s right/RF	LATCH w/o tether	32.8/20.4	31.1/19.3	31.7/19.7	24.0	140.4	161.0
DOT_SIDE_037	Cosco Scenera	Q3s right/RF	LATCH w/o tether	32.7/20.3	31.1/19.3	31.5/19.6	22.5	161.4	165.0
DOT_SIDE_038	Combi Zeus 360	Q3s left/FF	LATCH	32.8/20.4	31.2/19.4	32.0/19.9	22.9	159.0	167.0

Table 11: ATD response for tests DOT_SIDE_027 and DOT_SIDE_028

TEST NUMBER	CHILD RESTRAINT SYSTEM	ATD TYPE/ DIRECTION	IMPACT SPEED TO DOOR (kph/mph)	HEAD CONTACT	MAX RESULTANT HEAD ACCEL (g)	HIC 15/36	MAX SHOU LDER DISP (mm)	MAX IR-TRACC DISP (mm)	MAX RESULTANT UPPER SPINE ACCEL (g)	MAX PUBIC FORCE (N)	MAX RESULTANT PELVIC ACCEL (g)
DOT_SIDE_027	Graco Classic Ride 50	Q3s FF	31.4/19.5	yes	112.5	819/819	21.7	23.8	106.6	41.7	112.7
DOT_SIDE_028	Graco Classic Ride 50	Q3s FF	31.4/19.5	yes	106.2	790/790	22.5	24.1	106.1	44.9	122.9

Table 12: ATD response for tests DOT_SIDE_029 to DOT_SIDE_033

TEST NUMBER	CHILD RESTRAINT SYSTEM	ATD TYPE/ DIRECTION	IMPACT SPEED TO DOOR (kph/mph)	HEAD CONTACT	MAX RESULTANT HEAD ACCEL (g)	HIC 15	HIC 36	MAX RESULTANT CHEST ACCEL (g)	MAX RESULTANT PELVIC ACCEL (g)
DOT_SIDE_029	Combi Shuttle	CRABI12 RF	31.4/19.5	yes	80.5	359	359	65.2	116.9
DOT_SIDE_030	Combi Shuttle	CRABI12 RF	31.5/19.6	yes	79.0	386	386	83.1	141.1
DOT_SIDE_031	Evenflo Discovery 5	CRABI12 RF	31.7/19.7	yes	47.2	166	197	78.3	150.4
DOT_SIDE_032	Evenflo Discovery 5	CRABI12 RF	31.7/19.7	yes	49.7	178	214	68.5	129.6
DOT_SIDE_033	Evenflo Discovery 5	CRABI12 RF	31.5/19.6	no	48.6	178	217	77.1	130.6

Table 13: ATD response for tests DOT_SIDE_034 to DOT_SIDE_038

TEST NUMBER	CHILD RESTRAINT SYSTEM	ATD TYPE/ DIRECTION	IMPACT SPEED TO DOOR (kph/mph)	HEAD CONTACT	MAX RESULTANT HEAD ACCEL (g)	HIC 15/36	MAX SHOULDER DISP (mm)	MAX IR-TRACC DISP (mm)	MAX RESULTANT UPPER SPINE ACCEL (g)	MAX PUBIC FORCE (N)	MAX RESULTANT PELVIC ACCEL (g)
DOT_SIDE_034	Graco Classic Ride 50	Q3s RF	31.4/19.5	yes	104.5	702/702	18.6	26.5	95.8	705.7	120.7
DOT_SIDE_035	Graco Classic Ride 50	Q3s RF	31.2/19.4	yes	98.6	660/660	18.9	26.2	104.1	676.9	117.4
DOT_SIDE_036	Cosco Scenera	Q3s RF	31.1/19.3	yes	92.7	681/681	19.6	22.9	103.4	875.5	124.1
DOT_SIDE_037	Cosco Scenera	Q3s RF	31.1/19.3	yes	92.8	676/676	19.3	22.6	99.2	700.0	126.9
DOT_SIDE_038	Combi Zeus 360	Q3s FF	31.2/19.4	no	87.6	633/633	not recorded	not recorded	not recorded	not recorded	141.3

8.0 Observations

Per contract DTNH22-11-R-00204 Modifications III to V, the Kettering University Crash Safety Center was tasked and completed the following objectives:

1. Modified the side impact test fixture to address design issues identified during Phase I tests;
2. Conducted 15 baseline tests to assess the viability of the modifications of the fixture, the pre-impact kinematics of the anthropomorphic test device (ATD) head, and the measurement of the impact speed of the secondary carriage with the door fixture;
3. Conducted deceleration sled tests to assess repeatability;
4. Conducted 8 child restraint system (CRS) specific tests with a secondary carriage weight of 102 kg (225 lb);
5. Conducted 6 baseline tests to assess the secondary carriage acceleration and velocity time history with varying secondary carriage weight, aluminum honeycomb volume, and impact plane alignment;
6. Conducted 12 CRS specific tests with a secondary carriage weight of 116 kg (256 lb); and
7. Analyzed, transferred, and reported the test data.

The following observations were discerned during the study:

- The side impact test fixture was successfully modified to include an alternate anti-rebound mechanism, solid support structure for the aluminum honeycomb, uniform honeycomb impact plate, modified seat back pan, and raised lower anchor attachment points.

- The original prescribed springs for the new anti-rebound mechanism were changed out with longer springs after the device failed to catch the secondary carriage on rebound.

- The changes to the aluminum honeycomb support structure and the honeycomb impact plate functioned as designed. The struck honeycomb material deformed uniformly with the crush primarily on the impacted end. Also, the resulting crush was regular for consistent impact speeds, with 135 mm (5.3 in) of crush recorded for an impact velocity of 31.3 kph.

- When the ATD head was allowed to move with no restriction during the 800 mm run-up prior to CRS impact, the head had a maximum forward linear displacement of 85 mm (3.3 inches). Prior to impact of the CRS with the door, the head moved rearward 10 mm (0.4 inches) from this maximum position.

- Tests were conducted with masking tape secured to the head of the ATD on one end and the back of the CRS on the other. During the test, the tape tightened and stretched, allowing the head to move forward. In one test, the tape broke prior to impact. In another test, the tape came unsecured from the seat back prior to impact. In the other 5 tests, the tape stayed secure and broke at impact of the CRS to the door. When the tape did stay secure, the head rebounded from the maximum forward position.

- With the head taped or untaped, the ATD head flexed forward and rebounded during the 800 mm run-up from the initial staged position to impact with the foam door face. Therefore, the position of the ATD head at maximum engagement of the CRS to the door was similar for both test configurations.

- When using a deceleration sled to conduct the side impact test, the 19.5 mph impact speed of the CRS to the door was 0.8 mph less than the impact speed of the deceleration sled to the decelerator.

- Various methods for determining impact speed were used. The GHI Systems VS200 Velocimeter (one-pass optical sensor) provided the most consistent secondary velocity reading among the sensors evaluated and served as a confirmation tool for assessing the secondary carriage velocity as determined with integration of the acceleration data.

- When the only change to the test is speed, the acceleration time history depicts a combination of both the reduction of acceleration amplitude and time duration. And, the rate of change of the relative velocities is comparable between the tests.

- As the weight of the secondary carriage was increased, the peak acceleration decreased and the duration of the pulse increased.

- Variation to the weight being tested (payload which includes child restraint and dummy) on the secondary carriage has a nominal effect on the amplitude and duration of the secondary carriage pulse.

- The greater the volume of the honeycomb, the greater the peak acceleration of the pulse.

- Aligning the impact planes (honeycomb-to-carriage and door-to-CRS) has a nominal effect on the amplitude and duration of the secondary carriage pulse.

- Aligning the impact planes (honeycomb-to-carriage and door-to-CRS) alters the impact environment of the CRS.

- CRS side impact testing using a deceleration sled was demonstrated to be repeatable.

Appendix A

Calculation of Relative Velocity

1. Determining the velocity at which the primary carriage impacts the decelerator
    A. Using the complete acceleration data file for the primary carriage channel 00SLED000001ACX integrate the acceleration curve setting the speed of the carriage to 0.0 m/s at -3400 msec. Filter class CFC180 is used.
    B. Determine from the plot created in Section 1A, the velocity (m/s) at which the primary carriage contacts the decelerator. The point-in-time is defined as "time zero" and is defined by a trigger switch on the decelerator. (Figure A1)

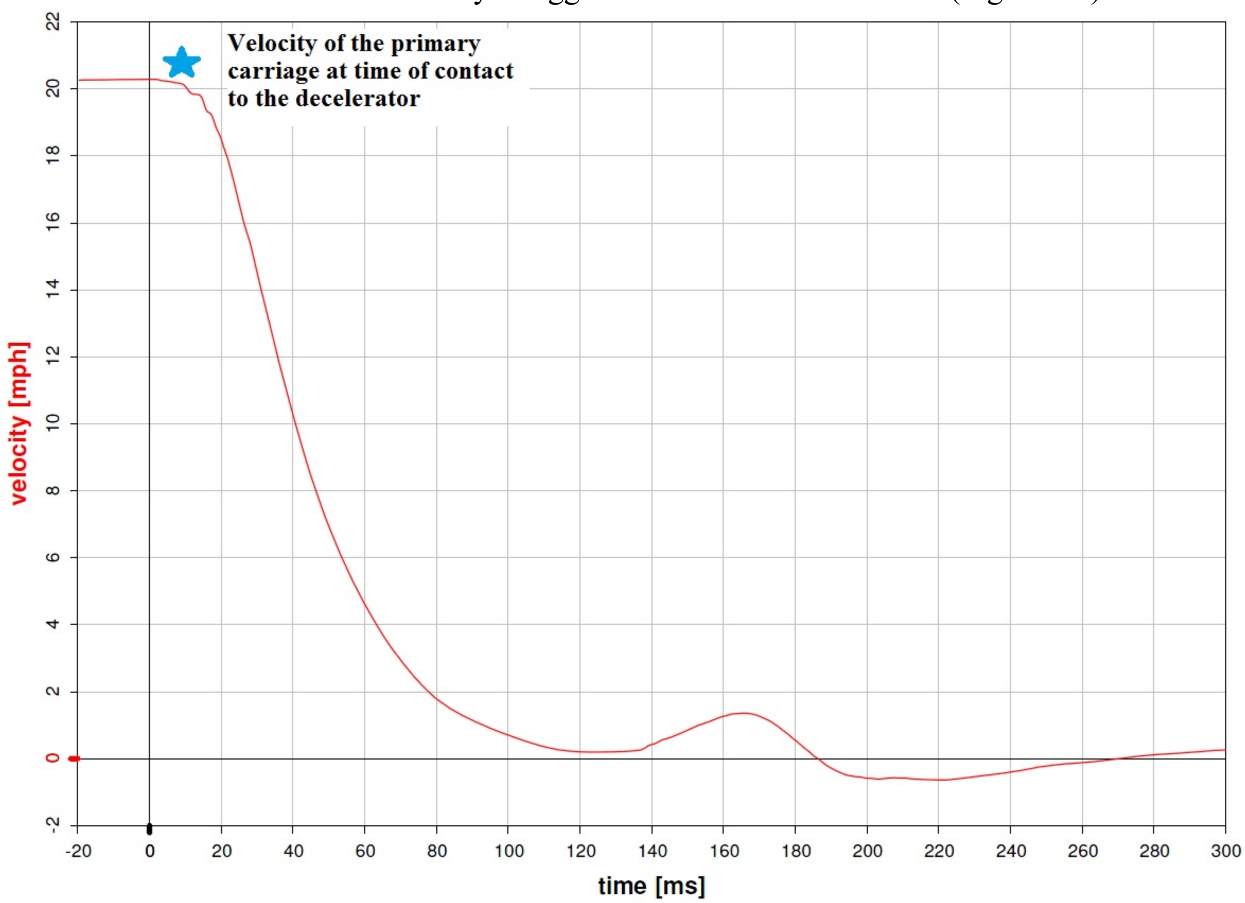

Figure A1: Integration of the primary carriage acceleration

2. Determining the speed of the secondary carriage
    A. The speed determined in Section 1B is the same as the speed of the secondary carriage along the longitudinal sled axis at "time zero."
    B. Multiply the speed in Section 1B by the cos10 (.9848) to determine the speed of the secondary carriage along the 10º track at "time zero" (contact of the primary carriage with the decelerator).
    C. Integrate the acceleration of seat back channel 00SLED000003ACX setting the speed (m/s) calculated in Section 2B as a fixed value at "time zero." Filter Class CFC180 is used.
    D. Determine from the plot calculated in 2C, the speed of the secondary carriage at impact with honeycomb/door. The point-in-time is defined by the inflection point

of the deceleration signal (contact of the secondary carriage aluminum plate to the honeycomb) (Figure A2).

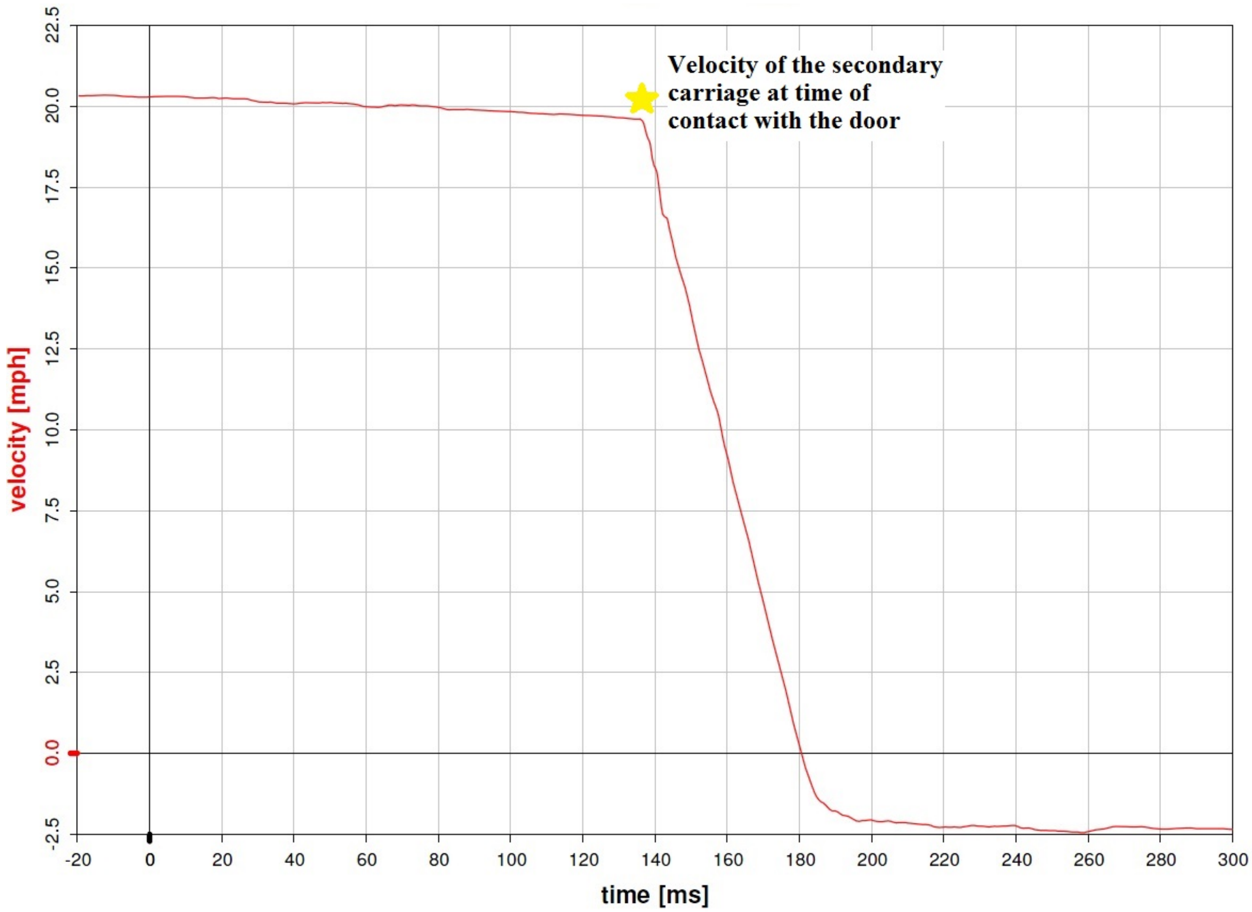

Figure A2: Integration of the secondary carriage acceleration

3. Determining the relative velocity
   A. Subtract the velocities of the two carriages along the 10º track [secondary carriage (channel 00SLED000003ACX)] - primary carriage (channel 00SLED000001ACX) * (cos10)]. As previously stated, filter class CFC180 is used for the velocity calculations.
   B. Determine from the plot calculated in 3A, the speed of the secondary carriage at impact with the primary carriage, the inflection point of the relative velocity signal (contact of the secondary carriage aluminum plate to the honeycomb). This speed should equate to the speed determined in Section 2D since the primary carriage should have reached 0.0 m/s velocity prior to the impact of the secondary carriage (Figure A3).

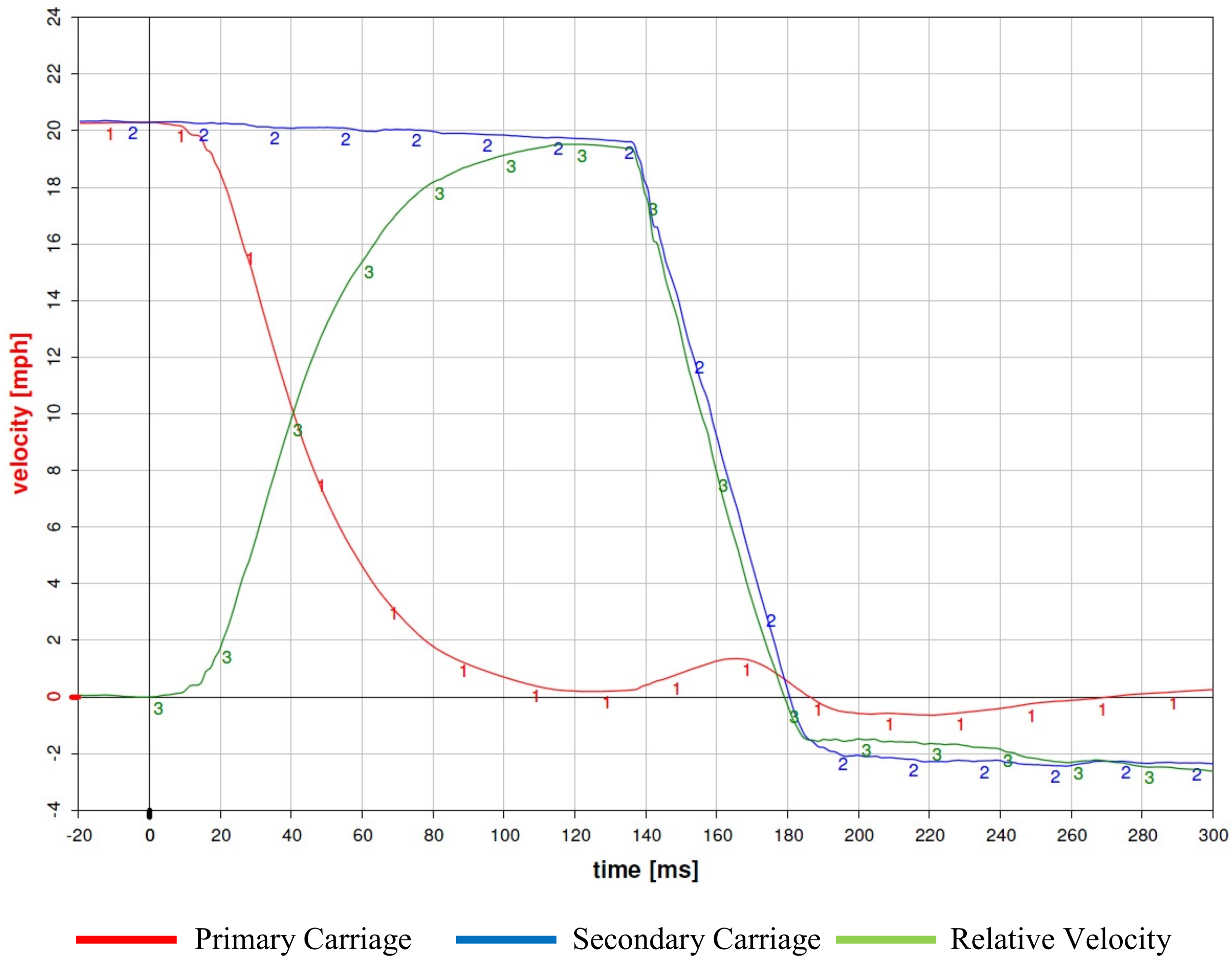

Figure A3: The relative velocity of the secondary carriage perpendicular to the door surface and time of contact.

Appendix B

Deceleration Sled Side Impact Test Procedure

Initial Setup

The side impact fixture consists of two distinct parts: the primary carriage and the secondary carriage (Figure B1). The primary carriage is fixed to the bedplate of the deceleration sled and consists of the fixture base plate, door fixture (with foams), and aluminum honeycomb. The secondary carriage is free to move on a set of linear bearings affixed to the primary carriage base plate at a 10 degree angle counter clockwise from longitudinal. The secondary carriage consists of the generic vehicle seat (with foam and cover), the child restraint system (CRS) being tested, and the anthropomorphic test device (ATD). The (final) mass of the secondary carriage is 116 kg (256 lbs). The properties of the fixture materials are listed in Table B1.

Figure B1: Front view of side impact fixture attached to the deceleration sled

Table B1: Properties and dimensions of fixture materials

Part	Material Properties and Dimensions
Door foam backing	Ethafoam 220 51 mm ± 3 mm (2.0 in ± 0.1 in) thickness, Figure B2
"Armrest" door foam	Four (4) pound gray foam from United Foam (UF) 64 mm ± 3 mm (2.5 in ± 0.1 in) thickness, Figure B2
Door foams attachment	3M two-sided foam mounting tape
Aluminum honeycomb	Plascore PAMG-XR1 5052 305 (depth) x 343 x 127 mm ± 6 mm (12"x13.5"x5" ± 0.1")
Bench foam and covering	Standard ECE R-44

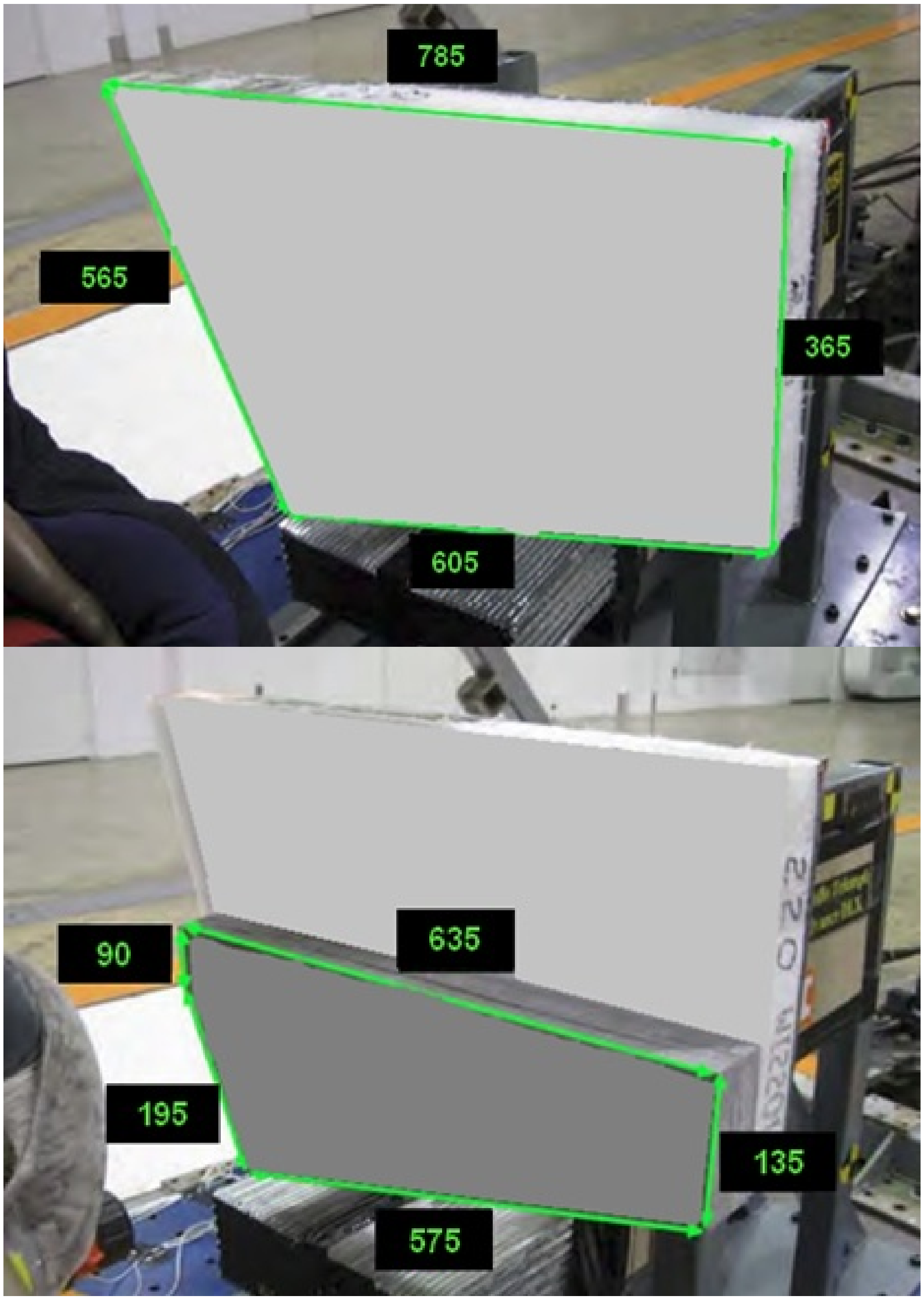

Figure B2: Door foam dimensions (mm) ± 6 mm

Instrumentation: Fixture and Sled

Sixteen channels of instrumentation are affixed to the deceleration sled and test fixture (Table B2). Locations of the accelerometers on the test fixture are shown in Figure B3. A strobe light is used and triggered by the secondary carriage impact into the aluminum honeycomb block. Its output is visible in all camera views.

Table B2: Sled and fixture instrumentation

Position of Measurement	Type of Measurement	Number of Channels
(1)* Primary carriage A_x	Linear acceleration	1
(2) Primary carriage A_x, A_y, A_z	Linear acceleration	3
(3) Bench seat back A_x, A_y	Linear acceleration	2
(4) Bench seat base A_x	Linear acceleration	1
Velocity secondary carriage (bench seat) t	time	1
(6) Rigid wall on primary carriage A_x, A_y	Linear acceleration	2
(7) CRS back A_x, A_y, A_z	Linear acceleration	3
Top tether (when applied) F_z	Axial belt force	1
Head contact indication switch V	Voltage	1
Honeycomb contact indication switch V	Voltage	1
Total instrumentation on sled and fixture		**16**

* Numbers correspond to labels on Figure B3

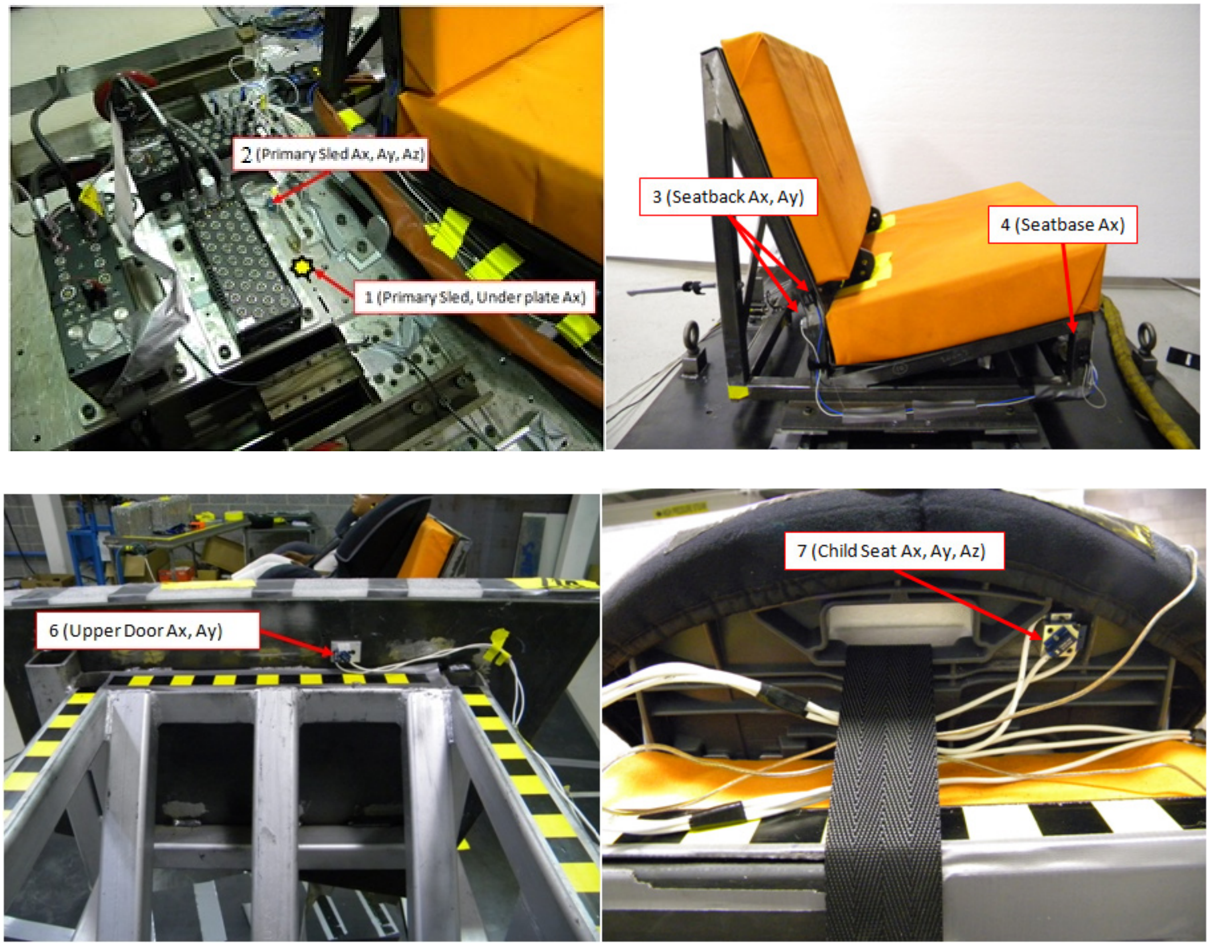

Figure B3: Instrumentation locations

Instrumentation: ATD

Two different ATDs are used in the side impact testing: CRABI 12 and Q3s. The instrumentation for the ATDs is listed in Table B3. All instrumentation is calibrated in accordance to the protocol specified in NHTSA "Laboratory Test Procedure for FMVSS No. 213, Child Restraint Systems" (TP-213-09 June 7, 2006). The CRABI 12 is clothed as specified in TP-213-09. Copper mesh is placed over the ATD's head (Figure B4) for use with the door contact switch.

Table B3: ATD instrumentation

Instrumentation Channel	**Q3s (number of channels)**	**CRABI 12 (number of channels)**
Head triaxial accelerometer (cg) A_x, A_y, A_z	3	3
Neck upper load cell Forces Fx, Fy, Fz Moment Mx, My, Mz	 3 3	 3 3
Shoulder displacement D_y	1	-
Chest triaxial accelerometer A_x, A_y, A_z	-	3
IR-TRACC displacement D_y	1	-
Spine triaxial accelerometer A_x, A_y, A_z	3	-
Lumbar spine load cell Forces Fx, Fy, Fz Moment Mx, My, Mz	 3 3	 3 3
Pubic force F_y	1	-
Pelvis triaxial accelerometer (cg) A_x, A_y, A_z	3	3
Total	**24**	**21**

Figure B4: CRABI 12 and Q3s heads prepared for testing with targets, copper mesh cover, and test chalk

High-Speed Video and Photography

There are five off board cameras specified for the side impact testing (Table B4). A layout showing the location of the cameras for forward facing and rear facing tests is provided in Figures B5 and B6, respectively. The camera speed setting is 1,000 frames per second for all cameras.

Placards are attached to various positions on the fixture such that they can be seen in each camera view during the duration of the event. Placard information includes test number, child seat manufacturer and model, CRS attachment method, ATD type, and ATD position.

Table B4: Camera information

Camera Location	Lens
Overhead 1 (Wide View)	20 mm
Overhead 2 (Tight View)	6 mm
Front	12 mm
In-Line with Secondary Carriage	3.5 mm
Front Oblique (Forward Facing) or Door Surface (Rearward Facing)	12 mm

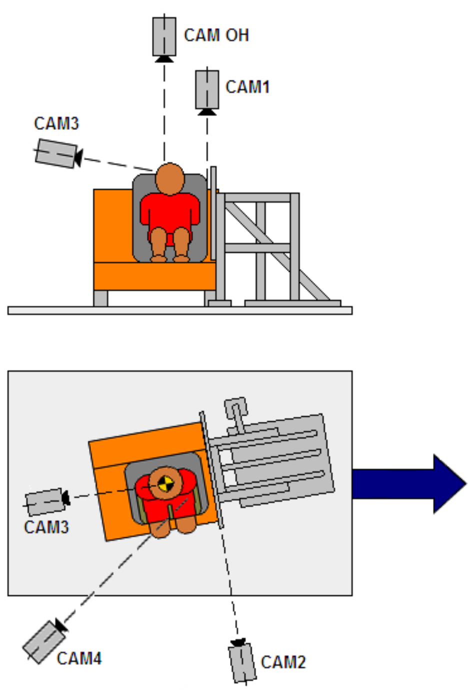

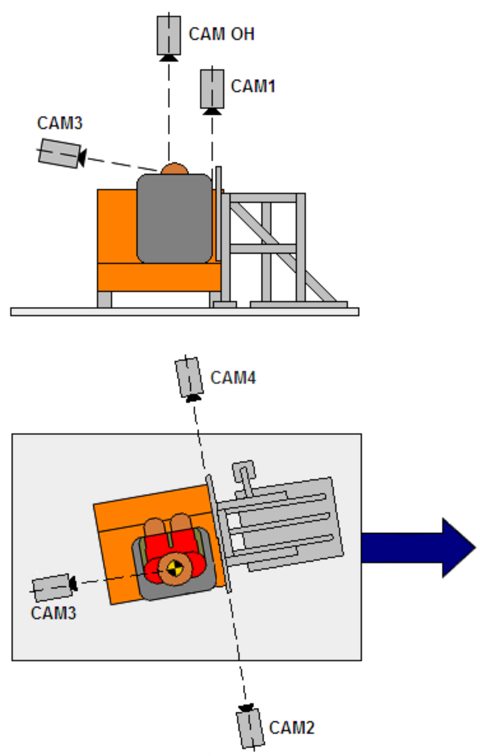

Figure B5: Camera positions for forward facing Figure B6: Camera positions for rear facing

Fixture and ATD Placement

- Fixture seat foam should be unloaded (allowed to rest) for a minimum of four hours prior to testing.
- Position the secondary carriage 800 mm ± 6 mm from the honeycomb impact surface (Figure B7). The 800 mm distance may be longer or shorter depending on the type of sled mechanism being used.
- Apply inch tape and targets to the appropriate areas on the CRS. Adjust the internal harness and center buckle positions according to the CRS owner's manual corresponding with the ATD size. Record the make, model, and serial number of the CRS.
- Position the CRS on the sliding seat 300 mm ± 6 mm from the edge, centered with the LATCH anchors. (Figure B7) For rear facing CRS, ensure the seat inclination meets manufactures specifications.
- Install ATD with the upper arms aligned with the torso and the hands resting on the CRS seat cushion. Route the data umbilical along the side of the ATD leg (opposite of impact) between the CRS side interior and the ATD. Position ATD so that the torso is in contact with the back of the seat and the top of the head aligned with the center targets on the top and bottom of the CRS. Position the thighs so they are equally spaced from the buckle and contacting the CRS seat bottom. Buckle and tighten the CRS internal harness. If using the Q3s ATD, ensure that the arm is positioned in the detent at approximately 25^0 angle with respect to the IR-TRACC.
- Tighten the internal harness, lower anchor attachments, and (when applicable) the upper tether, according to installation guidelines "Laboratory Test Procedure for FMVSS No. 213, Child Restraint Systems" (TP-213-09 June 7, 2006). Using a belt tension gauge, measure (and record) belt tension values for all three belt restraints. Target belt loads are listed in Table B5.
- Apply chalk paint to the ATD's head. Use different colors to distinguish front, side, and top of head.
- Attach new door and armrest foam to the steel door frame using two sided tape. Measure and record the distance from the rear of the honeycomb backing plate to the front impact plane of the armrest foam. (Figure B8)
- Apply contact foil to the door in a space appropriate for either forward facing or rear facing CRS.
- Apply test information placards to the foam.
- Attach the honeycomb to the honeycomb support structure.
- Fixture seat foam should be inspected for damage after each test and replaced as needed.

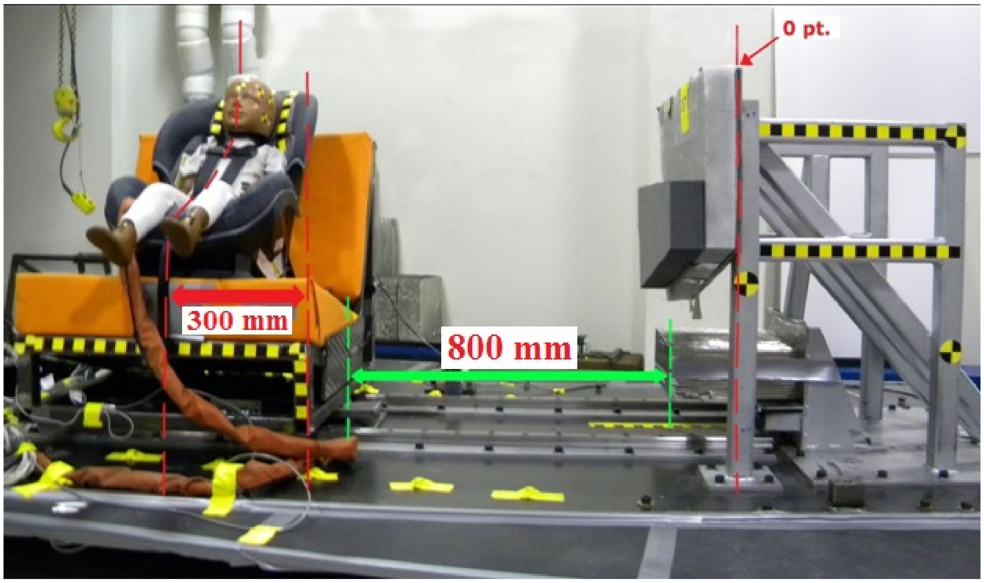

Figure B7: Pretest fixture dimensions

Table B5: Restraint system belt loads

Restraint	Target Load (lbs)
Internal Harness	1.5 to 3.0
Lower Latch Anchors	12.0 to 15.0
Upper Tether	9.0 to 12.0

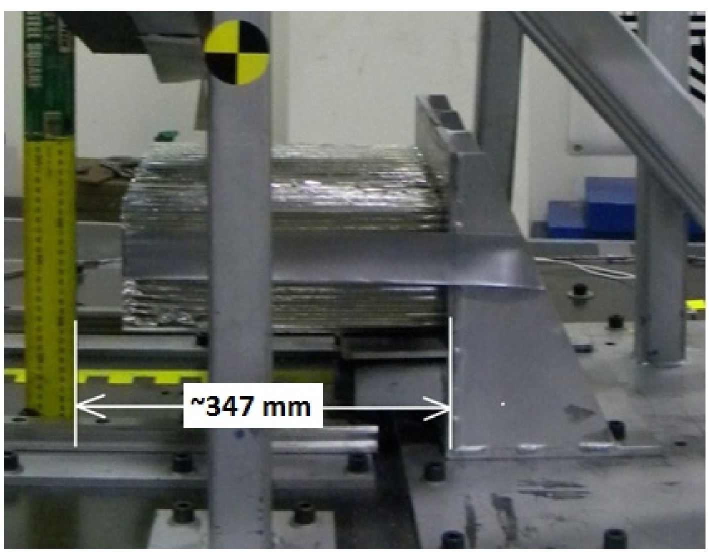

Figure B8: Pretest door surface to honeycomb support surface dimension

Coordinate Measurement Machine (CMM) Pre-Test Measurements

Using a CMM such as a FARO arm, measurements of the pre-test CRS, fixture, and ATD position are recorded. Table B6 lists the desired measurements. Sample measurements are shown in Table 7. The reference point (or origin) is the upper right corner of the door plate (Figure B7). CMM measurement locations are depicted in Figure B9. Measurements locations will vary for different ATDs and CRS. Though, the Y-axis measurement is the critical one to replicate, between CRS models for each dummy, to ensure that the CRS is aligned properly on the seat and that the dummy is aligned properly in the CRS.

Table B6: CMM measurements

Part	Measurement Position
Fixture	Secondary carriage seat forward corner
Fixture	Top forward corner of honeycomb
CRS	Top of seat
CRS	Center of seat base
CRS	Side of base
CRS	Side of CRS
CRS	Center of chest clip
CRS	Center of buckle
ATD	Top of head
ATD	Left head CG
ATD	Front of face
ATD	Left elbow (forward facing)/Right elbow (rear facing)
ATD	Top centerline of right knee
ATD	Top centerline of left knee

Table B7: Sample CMM measurements

Position	Index*	X (mm)	Y (mm)	Z (mm)
Seat base front centerline	1	-181.152	1197.822	414.547
Side of base	2	-445.925	1066.049	447.472
Side of seat	3	-458.33	1027.522	348.822
Top of seat	4	-853.567	1197.024	-54.54
Top of head	5	-702.345	1196.209	-95.542
Front of face	6	-593.287	1199.847	-38.057
Chest clip	7	-538.022	1195.012	80.292
Buckle	8	-404.059	1198.687	224.522
Left knee top	9	-279.2	1111.804	207.779
Right knee top	10	-272.85	1285.074	202.619
Left head CG	11	-680.102	1128.972	-17.912
Elbow	12	-527.114	1078.829	167.254
Sliding seat corner	13	-159.294	893.844	579.759
Honeycomb corner	14	-322.072	82.439	605.087

* Index numbers correspond to Figure B9

Figure B9: Layout of sample CMM measurement locations

Still Photographs

Pre and post test still photographs are taken per the list in Table B7. Placard information labels should be visible in all still photographs. Placard information includes test number, child seat manufacturer and model, CRS attachment method, ATD type, and ATD position. "Pre" or "post" test label should also be visible.

Table B7: Still photography locations pre- and post-test

Photo Location / Description	Pre	Post
Front overall	X	X
Front close-up of the ATD in the CRS	X	X
Left	X	X
Left oblique	X	X
Right	X	X
Right oblique	X	X
Rear	X	X
Overhead of sled buck with the CRS and placard in view	X	X
Child seat accelerometer attachment	X	
Close-up photo of CRS to document where all targets are on the CRS	X	
Manufacture label(s)	X	
Overhead view of close-up of impact plane		X
Test photo of chalk marks on seat and door		X
Honeycomb crush with measurement		X
Any damage on CRS (with or without fabric cover)		X
Any damage to test fixture		X

DOT HS 811 995
May 2014

U.S. Department
of Transportation

**National Highway
Traffic Safety
Administration**

www.nhtsa.gov

10219-050114-v2